AN ABSTRACT OF THE THESIS OF

GLEN ORVAL KLOCK for the Doctor of Philosophy
(Name) (Degree)

in Soils presented on December 7, 1967
(Major) (Date)

Title: PORE SIZE DISTRIBUTIONS AS MEASURED BY THE MERCURY INTRUSION METHOD AND THEIR USE IN PREDICTING PERMEABILITY

Redacted for privacy

Abstract approved: _____
(Larry Boersma)

A number of investigators have proposed equations to predict the permeability of porous media. Most of their equations are based on the distributions of the sizes of the various contributing pores in the medium. Presently the pore size distributions of agricultural soils are most commonly obtained from soil water release curves. The pressure scale is converted into an equivalent pore diameter scale by means of the pressure of displacement equation. This method is time consuming.

The study reported in this thesis was initiated to (1) use a mercury intrusion method to obtain pore size distributions of porous materials similar to agricultural soils, (2) use the pore size distributions thus obtained with existing equations to calculate intrinsic permeability and (3) compare the calculated permeability values with measured values for a range of particle size distributions.

The permeabilities and the pore size distributions of 54 systematically selected particle size classes of glass beads and crushed quartz sand were measured. The particle size classes ranged from 44 to 246 microns in diameter. The pore size distributions were evaluated and used in Marshall's proposed permeability prediction equation. The measured permeabilities did not agree with the calculated values until a correction factor which is a function of the pore diameter was used.

It is apparent that the pressure of displacement equation measures only an effective pore dimension. Permeability prediction equations require the evaluation of an effective hydraulic dimension. These two dimensions are different and are influenced by the geometry of the pore aperture. A necessary correction factor has been developed which accounts for the difference between the measured and hydraulic dimension when the mercury intrusion technique is used to measure pore size distributions.

The results of this study have improved and given a better theoretical basis for permeability predictions equations.

Pore Size Distributions as Measured by the Mercury Intrusion Method and Their Use in Predicting Permeability

by

Glen Orval Klock

A THESIS

submitted to

Oregon State University

in partial fulfillment of
the requirements for the
degree of

Doctor of Philosophy

June 1968

APPROVED:

Redacted for privacy

Associate Professor of Soils

In Charge of Major

Redacted for privacy

Head of Department of Soils

Redacted for privacy

Dean of Graduate School

Date thesis is presented December 7, 1967

Typed by Carol Baker for Glen Orval Klock

ACKNOWLEDGMENT

This study has been done as part of a research grant from the Office of Water Resource Research, United States Department of the Interior under Project B-001-ORE of the Oregon Water Resource Research Institute and Project 788 of the Oregon Agricultural Experiment Station.

The author wishes to express his appreciation to Doctor Larry Boersma for his guidance in this research and for his assistance in the preparation of this thesis.

The author also wishes to thank Doctor R. H. Brooks and Doctor J. A. Vomocil for their consultations on the research problem.

Finally, the author is deeply appreciative for the encouragement and assistance of his wife, Kathy. Without her understanding patience and cooperation during the many nights and weekends spent on this study, the author could not have met the requirements for this degree.

TABLE OF CONTENTS

TABLE OF CONTENTS (Continued)

LIST OF TABLES

LIST OF FIGURES

LIST OF FIGURES (Continued)

LIST OF FIGURES (Continued)

PORE SIZE DISTRIBUTIONS AS MEASURED BY THE MERCURY INTRUSION METHOD AND THEIR USE IN PREDICTING PERMEABILITY

INTRODUCTION

Predicting the rate of movement of fluids under hydraulic gradients in porous media from the measurement of an intrinsic property of the medium has long been the goal of many investigators. The logical intrinsic property of the porous medium to use for the prediction of permeability is the pore aperture size distribution. The passage ways available in the porous medium for the fluids to pass through can be thought of as a randomly distributed array of pores in space, connected by channels of a specific aperture radius. Assuming the flow to be laminar in nature, the equations given by Poiseuille and Darcy can be applied. The prediction of the permeability of a porous medium then resolves itself into two problems, namely (1) the measurement of the pore size distribution and (2) the development of a procedure by which the permeability may be calculated from the measured pore size distribution.

Presently, pore aperture size distributions for agricultural soils are obtained from soil water release curves. This method has some serious limitations (Hillel and Mottes, 1966). Replication of pore size distributions in homogeneous material can be difficult to obtain. Development of a technique to measure pore size distributions, first used by Drake and Ritter (1945) in their work with

chemical powders, may overcome many of the serious drawbacks of using liquid release curves. This technique employs the forcing of mercury, a non-wettable agent, into the porous material. Pore aperture size distributions are then obtained from the pressure of displacement equation and the volume of mercury forced into the porous material.

Several methods have been proposed by which the permeability may be calculated from a given pore size distribution. These methods are based on applications of the laws of Poiseuille and Darcy. The essential element of all methods is to give a procedure by which the contributions of flow through each pore can be estimated to obtain the total flow rate.

The aim of this dissertation is to (1) examine the mercury intrusion porosimeter as a tool for the measurement of pore aperture size distributions of agricultural soils and (2) compare permeabilities calculated on the basis of the pore aperture size distribution measurement with experimentally determined values.

This dissertation is one phase of a project established to predict permeabilities at all levels of saturation. Although the objective of this dissertation is only concerned with predicting saturated permeabilities, equipment was constructed and procedures established to continue research in the area of predicting permeabilities for unsaturated porous media.

REVIEW OF LITERATURE

Pore Aperture Size Distribution of Agricultural Soil

In the investigation of soil water, a relationship is encountered between the water content of the soil and pressure deficiency, or suction, with which the water is held. This relationship gives the familiar soil water characteristic curves (Childs, 1945). These soil water characteristic curves, in turn, can show the pore aperture size distribution within the soil (Schofield, 1938; Leamer and Lutz, 1940; and Childs, 1940).

The pressure differential, P, required to maintain the soil at a given water content is the pressure difference across the air-water interface within the soil pores. If r is the radius of curvature of a spherical interface in equilibrium at this pressure difference, then the pressure of displacement equation states that

$$P = \frac{2\sigma \cos \theta}{r} \qquad (1)$$

where σ is the surface tension and θ is the contact angle between the liquid and the solid. Pores into which the interface retreats via channels of radius greater than r will, at this pressure deficiency, be theoretically emptied of all water except that which remains in the soil pores with an interface of smaller

radius of curvature. Pores into which the interface cannot retreat, except through channels of radius smaller than r, will remain full of water. As the water pressure increases the water content progressively decreases as a result of the successive emptying of pores of smaller and smaller radii. Thus, the pressure axis (x coordinate) of the soil water characteristic curve can be regraduated in terms of pore aperture size by means of equation (1). The y coordinate of any point on the water characteristic curve then gives the quantity of water held in pores of radius smaller than that given by the x coordinate.

The soil water characteristic curve then gives the distribution of the total pore space among pores of different sizes. Since the natural pores are very irregular in shape, the effective pore aperture size given by equation (1) bears a relation to the true pore aperture size which is of the same nature as the relation between effective and true particle diameter in mechanical analysis.

Soil water characteristic curves are determined by the methods proposed by Richards (1941). The soil water content of samples supported by a porous plate and subjected to a certain pressure is determined at equilibrium. Ceramic plates, sintered-glass plates, aluminum filter discs, cellophane membranes and other porous material have been used by different investigators (Nielsen and Phillips, 1958; Tanner, 1954; and Richards, 1941 and 1948) to retain

the soil sample as the soil water is removed by the application of a pressure. Although the importance of plate or membrane impedance is recognized (Miller and Elrick, 1958), the characteristics of the plate or membrane are generally assumed to have no influence on the soil water characteristic curve, provided the bubbling pressure of the porous plate or membrane is not exceeded.

The work of Jackson, van Bavel, and Reginato (1963) and Hillel and Mottes (1966) has shown that the porous plate or membrane does have an influence on the soil water characteristic curve. Their work also shows that soil water characteristic curves are influenced by the pretreatment of the soil sample and the time allowed for the sample to reach an equilibrium condition under a given pressure. All these factors are responsible for the lack of reproducibility in the measurement of soil water characteristic curves and in turn, pore aperture size distribution.

There are two fluids present in the soil sample subjected to pressure in a porous plate apparatus, namely water and air. The fluid which "wets" the solid in a "two-fluid" system is considered to have a contact angle against the solid less than 90 degrees. In the case of air and water as the two fluids, water is the wetting agent and has a contact angle of zero degrees. For the "wetting" fluid, the pressure difference across the interface is such that the fluid systematically fills the voids within the solid. This pressure

difference, likewise, opposes the removal of the fluid from the pores of the solid.

Drake and Ritter (1945) in studying the pore size distribution of catalysts, proposed a technique of using mercury to measure pore sizes. Purcell (1949) further developed this technique so that it might be applied to materials having pore sizes of the magnitude found in natural rock formations.

Pore aperture size distribution measurements by this technique involved the porous medium and a single "non-wetting" fluid (mercury) which forms a contact angle of approximately 140 degrees against a solid. In this case, the action of the surface forces involved opposes the entrance of the liquid into the solid and pressure must be applied to the liquid to cause penetration of the pores of the solid.

Purcell (1949) compared capillary pressure (which can be converted to equivalent pore radius by equation (1)) with the percent of total pore space occupied by both water and mercury for a number of different rock formations. He did find relatively close agreement between these curves for mercury and water/air over the range of porosities encountered. Purcell considered the saving of time for measuring a number of points on the capillary pressure curve as the chief advantage of the mercury intrusion method. Also, the range of capillary pressure or pore aperture sizes that can be measured is

considerably greater than that for the porous plate or membrane method.

Methods of Calculating Saturated Permeability

A considerable amount of work has been done attempting to obtain a useful relationship between pore aperture size distributions and permeability of porous materials. Several theories have been proposed for the calculation of permeability values from pore aperture size distribution data.

Purcell

Purcell (1949) with his mercury intrusion method of measuring capillary pressure curves or pore aperture size distributions was one of the first individuals to use this information to predict permeability of porous materials. This method has since been further developed by researchers in the petroleum industry. Purcell (1949) with the use of the pressure of displacement equation (equation 1); Poiseuille's equation

$$\frac{Q}{t} = \frac{\pi R^4 P}{8\eta L} \qquad (2)$$

where Q/t is the rate of flow of a fluid of viscosity, η, through a single cylindrical tube or capillary of length L, and internal

radius R, and P is the pressure drop across the tube; and Darcy's Law

$$\frac{Q}{t} = \frac{KAP}{\eta L} \tag{3}$$

where K is the permeability and A is the cross-sectional area of a flow system, developed the following equation for the permeability of a porous system

$$K_p = 0.66\ F\ f \int_{P}^{P=100} \frac{dp}{(P_c)^2} \ . \tag{4}$$

In equation (4), K_p is the permeability in millidarcies, f is the porosity in percent, p is the percent of total pore space occupied by the liquid, P_c is the capillary pressure expressed in atmospheres, and F is a "lithology" factor or matching factor to account for difference between the flow in a hypothetical porous medium and that in naturally occurring rocks. To obtain this equation a surface tension of 480 dynes per centimeter and a contact angle of 140 degrees for mercury is assumed.

Purcell's experimental data showed that the proposed equation provides a fairly reliable method of calculating permeability. The most serious disadvantage is the requirement for the "lithology" or matching factor.

Childs and Collis-George

Childs and Collis-George (1950) developed an equation to calculate the permeability from pore aperture size distribution data. They considered the porous medium to be an uncemented isotropic material with a randomly distributed array of pores in space, each of which is connected to other pores by channels. They assumed that all effective resistance to flow within a pore sequence is confined to the smaller pore or channel and that the only contribution to permeability is by a direct sequence of pores. Again, using Poiseuille's equation (equation 2) with its relationship between permeability and the radius of a tube, Childs and Collis-George derived a formula for permeability, K', which sums up the effect of all possible pore size sequences

$$K' = M \sum_{P=0}^{P=R} \sigma^2 f(\rho)d\rho f(\sigma)d\sigma \qquad (5)$$

where $f(\rho)d\rho$ is the area devoted to pores of radius ρ to $z+dr$ and $f(\sigma)d\sigma$ is the area devoted to pores in the range σ to $\sigma+dr$. The summation is stopped at the pore size, R, appropriate to the largest pore which remains full of water. The constant M, an apparent method to account for the tortuosity factor, is determined by matching calculated and experimental permeability curves at a

single point. The theory requires that the soil water characteristic curve be divided into a number of divisions of pressure values which in turn gives the pore aperture size distribution.

The direct use of the formula is quite involved and requires the experimental determination of one point on a permeability-pressure curve to evaluate the matching factor M. Thus, for saturated conditions alone the method can not be used to calculate permeability.

Marshall

Marshall (1958) developed an equation to calculate permeability from pore aperture size distribution data based on the same assumptions employed by Childs and Collis-George (1950). Marshall used the basic assumption that the rate of fluid flow through a porous medium is controlled by the cross-sectional area of the necks connecting the pores. The mean cross-sectional area of these necks can be taken to represent the cross-sectional area of a tube through which fluid flow occurs. According to Poiseuille's equation for laminar flow through a tube

$$v = \frac{-r^2 \frac{d\phi}{d\ell}}{8\eta} \qquad (6)$$

where v is the mean velocity for a fluid in a narrow tube of radius

r in which $d\phi/d\ell$ is the potential gradient causing flow and η is the viscosity.

By making the additional assumption that the fractional pore aperture or neck cross-sectional area in any plane is the same as the total porosity E, equation (6) becomes

$$v = \frac{-E\, r^2 \frac{d\phi}{d\ell}}{8\eta} \quad . \tag{7}$$

Equation (7) can be used to predict the rate of flow of a liquid in an isotropic porous material where all pore necks or pore apertures are of equal radius. Since this condition does not exist in porous materials, Marshall (1958) has given the following analysis as a correction for conditions where more than one pore aperture radius occurs.

> If the two surfaces, A and B, exposed by a section through an isotropic porous material are rejoined randomly, the pores on these surfaces will be connected by necks whose area of cross-section can be considered in the following way. The unit area of each of the exposed surfaces can be regarded as being made up of n portions each of the same area, $1/n$, and porosity E, and each containing pores of one mean radius $r_1, r_2, \cdots$ and r_n respectively, where $r_1 > r_2 > \cdots > r_n$. That portion of surface A which has pores of radius r will, in effect, contact "n" portions of surface B each of area $1/n$ and each containing pores of one size $r_1, r_2, \cdots$ and r_n respectively. The area of neck resulting from perfect pore to pore contact will be that of the smaller pore. However, the smaller pore can fit against more or less of the solid matrix instead of wholly against a pore on the opposite surface and, on the average, the area of contact will be E times the

area of the smaller pore. Hence, the mean neck area for each of the "n" portions of surface A will be $E\pi r_1^2$, $E\pi r_2^2$, $\cdots$ and $E\pi r_n^2$ respectively. Similarly that portion of A containing pores of size r will provide neck areas of $E\pi r_2^2$, $E\pi r_3^2$, $\cdots$ and $E\pi r_n^2$ respectively for another n portion of surface B (each of area $1/n^2$) with which it makes contact. The series is continued in this way until the n^{th} portion of surface A containing pores of radius r_n has been considered. This last portion will provide a neck area of $E\pi r_2^n$ for each of the n portions of surface B with which it makes contact. The average area of cross-section of neck for all the n^2 portions of surface B is then

$$A = E\pi n^{-2}[(r_1^2+r_2^2+\cdots+r_n^2)+(2r_2^2+r_3^2+\cdots+r_n^2) + \cdots + \pi r_n^2] \qquad (8)$$

or

$$A = E\pi n^{-2}[r_1^2+3r_2^2+5r_3^2+\cdots+(2n-1)r_n^2] \quad . \qquad (9)$$

Equation (9) gives the equivalent cross-sectional area of all pore necks contributing to liquid flow with an effective radius of r where

$$r_t^2 = En^{-2}[r_1^2+3r_2^2+5r_3^2+\cdots+(2n-1)r_n^2] \quad . \qquad (10)$$

Then, to determine the flow rate for a porous material with a distribution of pore apreture sizes, the effective radius is used

in equation (7) or

$$v = \frac{-E^2 \frac{d\phi}{d\ell}}{8\eta n^2} \Sigma[r_1^2 + 3r_2^2 + 5r_3^2 + \cdots + (2n-1)r_n^2]. \quad (11)$$

Equation 11 is a form of Darcy's law in which

$$v = -K' \eta^{-1} \frac{d\phi}{d\ell} \quad (12)$$

where K' is the permeability and

$$K' = \frac{E^2}{8n^2} \Sigma[r_1^2 + 3r_2^2 + 5r_3^2 + \cdots + (2n-1)r_n^2]. \quad (13)$$

Equation (13) is similar to equation (5) derived by Childs and Collis-George with an evaluation of the matching factor, M, based on Poiseuille's equation.

Marshall compared permeabilities calculated with equation (13) with those measured for the same porous materials and found good agreement. Several investigators (Millington and Quirk, 1959; Nielsen, Kirkham and Perrier, 1960; Schmidt, 1961; and Jackson, Reginato, and van Bavel, 1965) have compared permeabilities calculated with equation (13) with measured permeabilities and found considerable disagreement.

Millington and Quirk

Millington and Quirk (1959) proposed a modification of equation (13). Marshall (1958) assumed that the fractional pore area in any plane is of the same value as the porosity "E". Millington and Quirk showed that the effective pore area available for flow is proportional to "$E^{2/3}$" rather than being proportional to "E". With this modification they presented the following equation for calculating the intrinsic permeability.

$$K' = \frac{E^{4/3}}{8n^2} \Sigma[r_1^2 + 3r_2^2 + 5r_3^2 + \cdots + (2n-1)r_n^2] \quad (14)$$

To prove the validity of their equation they showed good agreement with experimental permeability values determined on very coarse sands (250 - 1,000 microns).

Jackson, Reginato, and van Bavel

Jackson, Reginato, and van Bavel (1965) compared the Childs and Collis-George, Marshall, and Millington-Quirk equations for 50-500 micron sand. They found that the Marshall equation matched the measured saturated permeability quite well. The Childs and Collis-George equation was not able to predict the saturated permeability because of the required matching factor. The Millington-Quirk equation over-estimated the saturated permeability. Jackson

et al. (1965) proposed using the ratio of measured to calculated permeabilities as a matching factor (0.606) with the Millington-Quirk method to predict permeabilities.

Laliberte

Another approach to predicting permeability from pore radius distributions was made by Laliberte (1966). Using the theory first proposed by Purcell (1949) and later used by Burdine (1953) and Wyllie and Spangler (1952), he showed a functional relationship between saturated permeability, effective porosity, bubbling pressure, and pore size distribution index. The pore size distribution index is a parameter developed by Brooks and Corey (1964) and is defined as the slope of the log-log plot of effective saturation as a function of capillary pressure. The bubbling pressure is a measure of the maximum pore size forming a continuous network of flow channels within the porous medium. Laliberte's equation for predicting saturated permeability, Ko, is written as

$$Ko = \frac{\phi_e \sigma^2 \cos^2\theta}{P_b^2 k T} \cdot \left(\frac{\lambda}{\lambda+2}\right) \qquad (15)$$

where ϕ is the effective porosity, σ is the surface tension, θ is the contact angle, P_b is the bubbling pressure, k is a shape factor, T is a tortuosity factor and λ is the pore size

distribution index. From experimental data Laliberte (1966) found that the error introduced by substituting a value of five for $kT/\cos^2\theta$ is less than 25 percent. Accepting this level of accuracy he was able to write the equation for saturated permeability

$$Ko = \frac{\phi_e \sigma^2}{5P_b^2} \cdot \left(\frac{\lambda}{\lambda+2}\right) . \qquad (16)$$

Laliberte used the value of five for $kT/\cos^2\theta$ as a mean value. He was not able to completely isolate its source of variation, but inferred that most, if not all, of the variation can be attributed to tortuosity.

MATERIALS AND METHODS

Porosimeter

Principles

The mercury intrusion method has been used extensively for the determination of pore size distributions of industrial materials. Purcell (1949) first used this method to obtain information needed for the prediction of permeability values from well drill cuttings in rock formations. With an establishment of a test procedure, this method could possibly be used for the determination of pore aperture size distributions of agricultural soils.

When mercury is forced into a pore in a solid material, the pressure required to fill the pore completely is inversely proportional to the size of the pore. This relationship, first pointed out by Washburn (1921), is shown in equation (1)

$$P = \frac{2\sigma \cos \theta}{r} \qquad (1)$$

where P is the pressure, r is the pore radius, σ is the surface tension of mercury, and θ is its angle of contact with the solid. Since σ and θ are both constants, application of a known pressure yields the corresponding pore dimensions. The mercury intrusion porosimeter is an instrument by which pressure can be

applied to a reservoir of mercury in contact with a porous solid sample. Precise measurement of changes in the volume of mercury as the pressure is increased provides a measure of the volume of pores in a given size range. Figure (1) shows a graph of mercury penetration in cubic centimeters as a function of pressure applied for two soil types - Chehalis loam and Ephrata loamy sand. Using a contact angle of 130 degrees and a surface tension of 473 dynes per centimeter in equation (1) for porosimeter data, the relation between pore diameter and pressure is

$$D = \frac{175}{P} \quad . \tag{17}$$

Thus, the pore diameter, D, is scaled along with the pressure applied in Figure 1.

Equipment

The equipment used was an Aminco-Winslow Porosimeter shown in Figure 2, which has a pressure range of 0-5,000 pounds per square inch, absolute. The sample is contained in a penetrometer assembly, shown in Figure 3, which is put into a filling device shown in Figure 4.

To make a measurement the penetrometer assembly is inserted into the filling device which is sealed and evacuated to a pressure less than 50 microns of mercury or 0.000065 atmospheres.

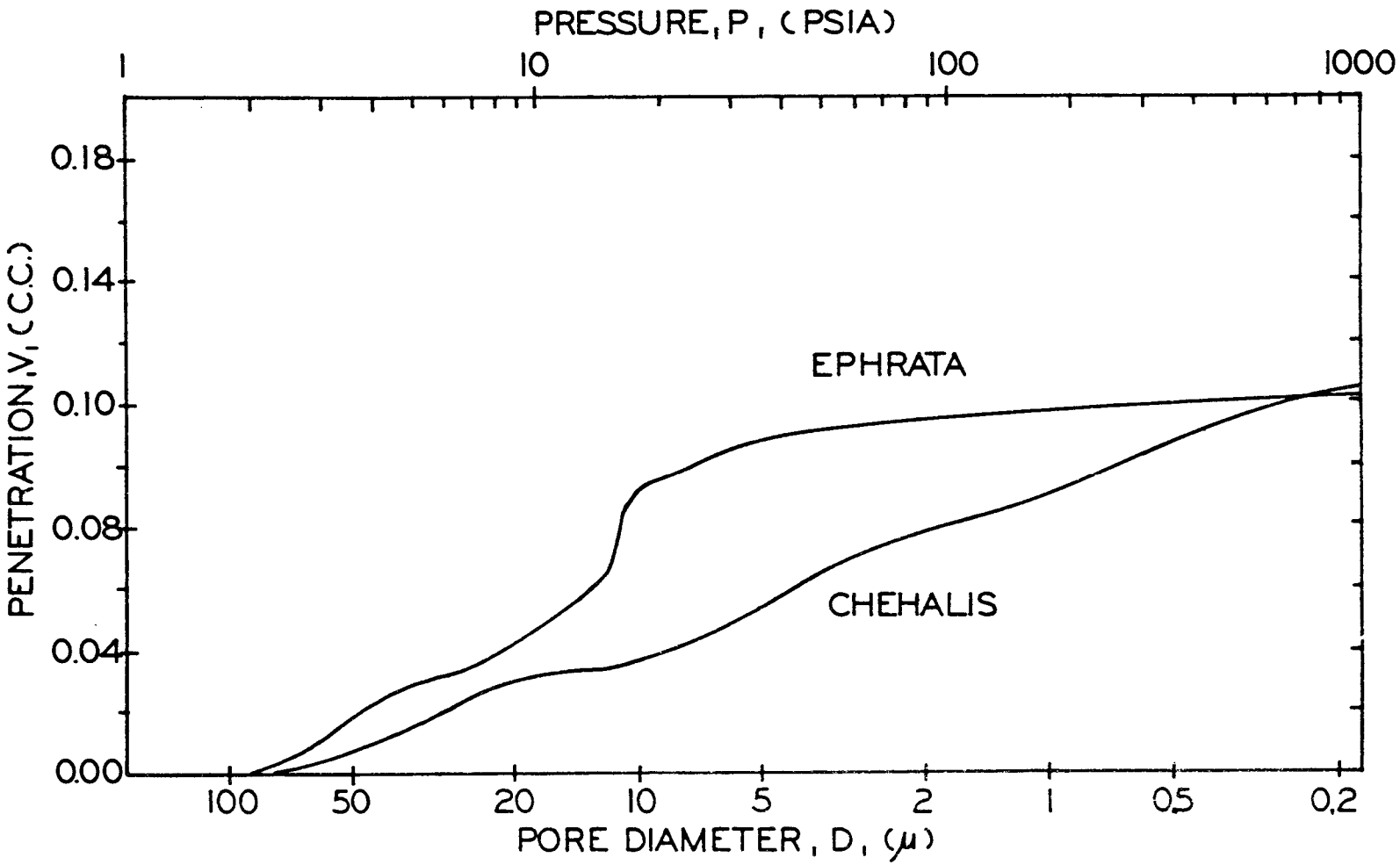

Figure 1. Pore size distribution determination for Ephrata loamy sand and Chehalis loam soil.

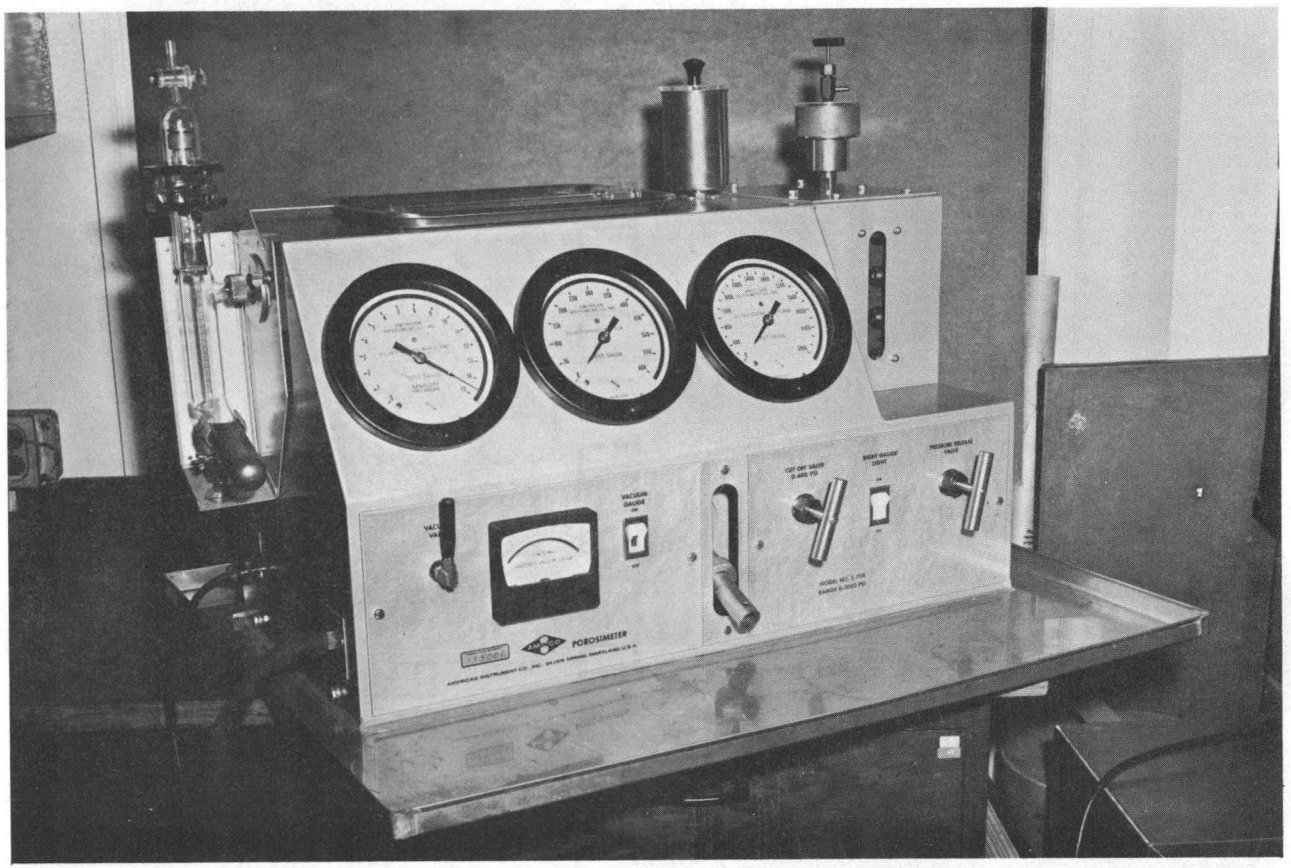

Figure 2. Front view of the mercury intrusion porosimeter.

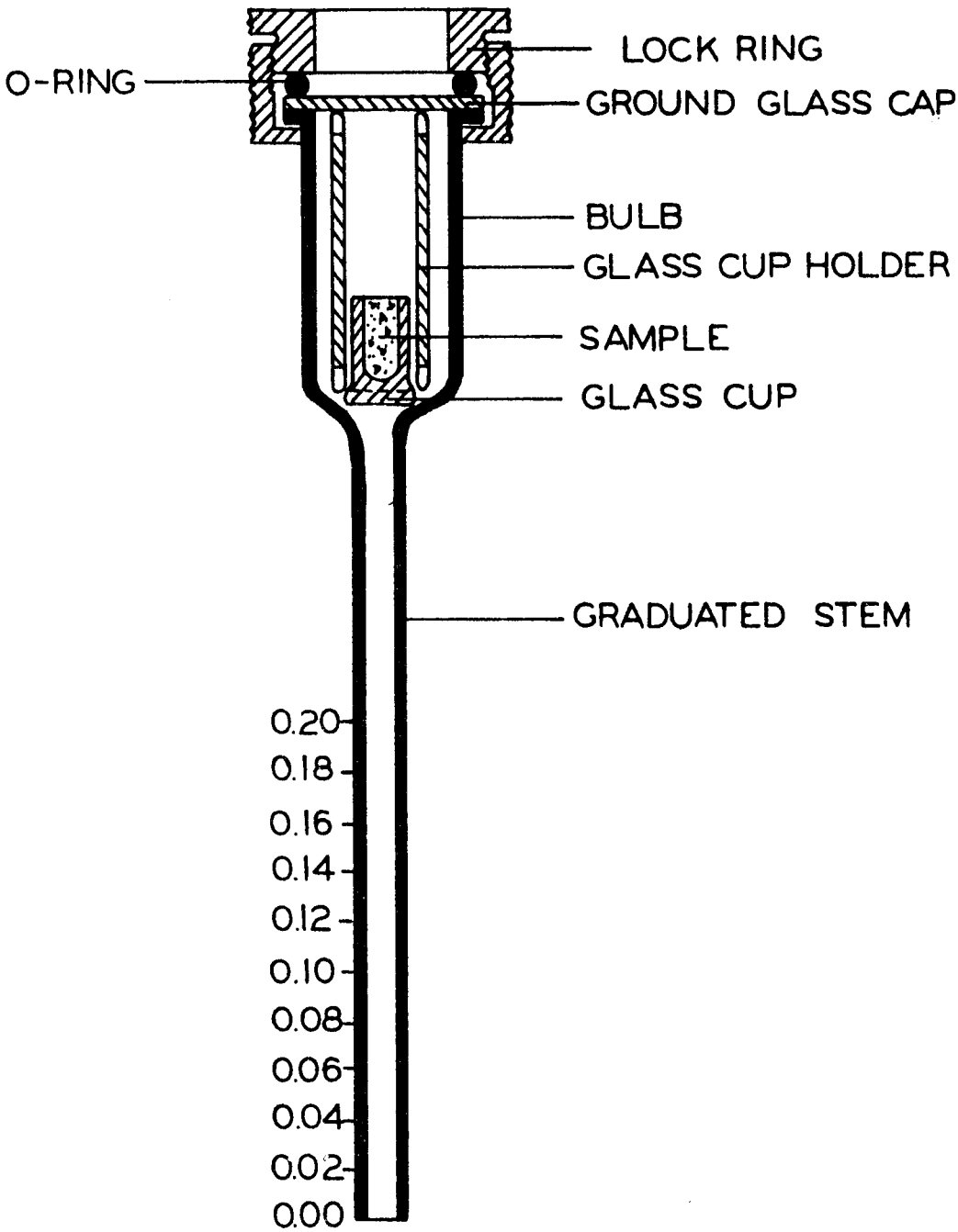

Figure 3. Mercury intrusion porosimeter penetrometer assembly.

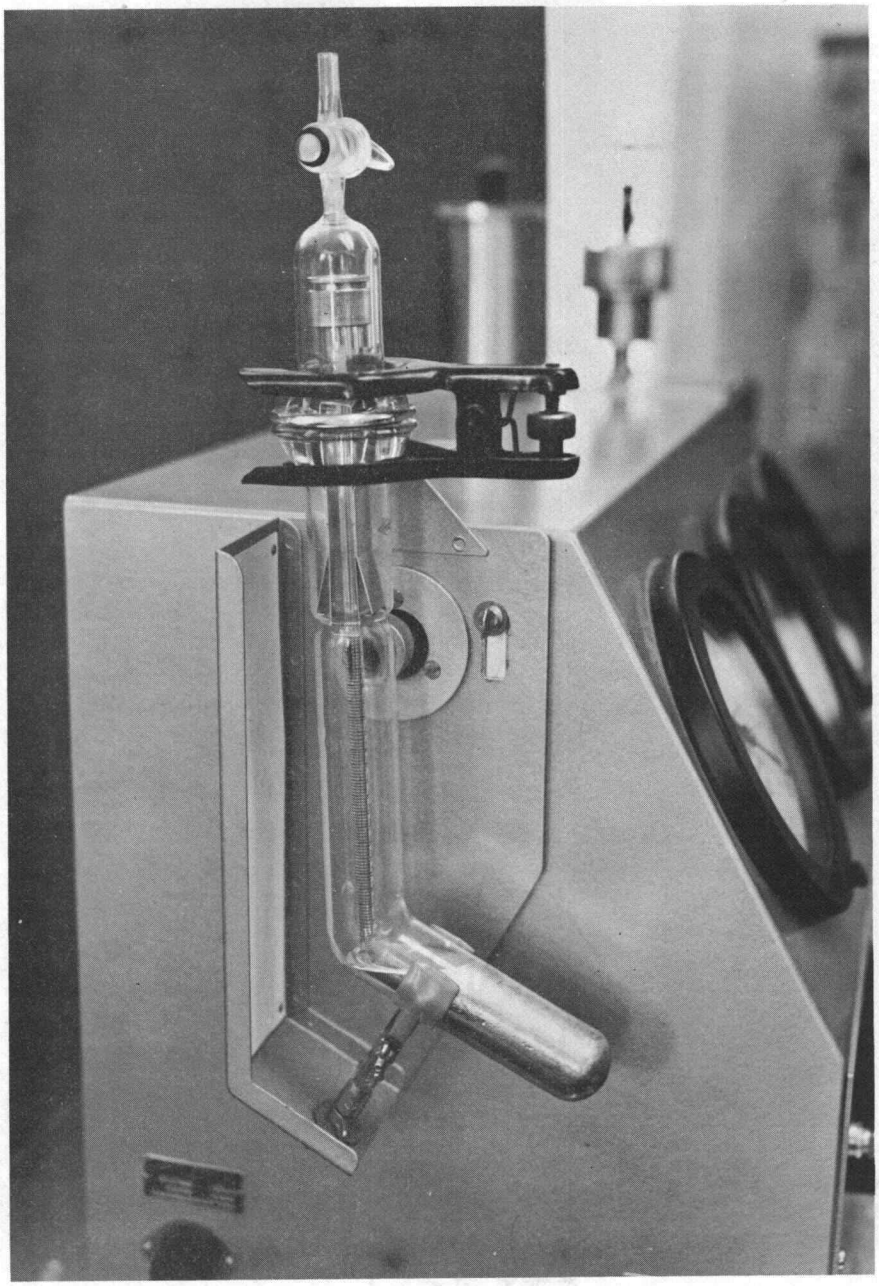

Figure 4. A side view of the filling device for the mercury intrusion porosimeter penetrometer.

Once this pressure is reached (usually about five minutes with a good vacuum pump), the lower tip of the penetrometer is immersed into the mercury pool in the bottom of the filling device by slightly tipping the entire filling device. Vacuum pumping is ceased and the pressure is allowed to increase to 6.0 pounds per square inch, absolute. This pressure is required to completely fill the penetrometer and limits the maximum measured pore radius to 60 microns. The pressure in the penetrometer assembly is increased up to atmospheric pressure step by step in approximate 0.5 pounds per square inch increments, and the pressure and stem reading recorded. At this point the penetrometer is removed from the penetrometer assembly and placed in a pressure vessel. Once again the pressure is increased by increments. Larger increments of pressure are used in the pressure vessel. The amount of pressure change is based on the rate of volume change in the penetrometer. For increased accuracy, increments of pressure applied should be used which change the column of mercury forced into the sample a small amount.

The penetrometer as manufactured by the Aminco-Winslow Company does not have the sample container shown in Figure 3. These sample containers or cups were made from glass tubing with an outside diameter of 0.8 centimeters and an inside diameter of 0.6 centimeters. The sample cup volume was calibrated with mercury.

To prevent tilting of the sample cups in the penetrometer bulb and to avoid spilling the material to be tested, cup holders were constructed as shown in Figure 4. The sample cups are needed for a determination and control of the total porosity of the sample. The maximum sample volume is controlled by the volume of the penetrometer stem (0.2 cc.) and the bulk density of the sample. For a range of bulk densities from 1.0 to 2.0 grams per cubic centimeter, the maximum bulk sample volume will vary from 0.32 to 0.87 cubic centimeters, assuming a particle density of 2.65 grams per cubic centimeter. To fill the sample cup, an extension was adapted to the cup and the porous material was poured into the assembly which was then tapped until the sample height in the extension remained constant. The extension was removed and the sample cup placed in the cup holder.

Calculation of Pore Aperture Size Distributions

An example of the calculations necessary to obtain the pore aperture size distributions from the readings obtained is shown in Table 1. The actual readings are recorded in colums (2) and (5) and are shown in parenthesis. The absolute pressure in the sample is obtained by subtracting from the gauge reading the weight of the mercury column. In order to make this conversion, a table was prepared showing the correction to be made corresponding to a certain penetrometer reading. This is reported as Table 2. The absolute

Table 1. Pore size distribution determination for quartz sand size class 115 with the mercury intrusion porosimeter.

1 Mercury Pressure (psi)	2 0-15 Gage Pressure (psi)	3 0-5000 Gage Pressure (psi)	4 Total Absolute Pressure (psi)	5 Penetrometer Stem Readings ($cm.^3$)	6 Functional Pore Value ($cm.^3$)	7 Percent Pore Value (%)	8 Pore Diameter (micron)
4.53	(6.0)		1.47	(0.000)	0.141	100	119.0
4.53	(8.0)		3.47	(0.001)	0.141	100	49.5
4.51	(8.5)		3.99	(0.002)	0.139	99	43.5
4.50	(9.0)		4.50	(0.003)	0.138	98	38.5
4.49	(9.5)		5.01	(0.004)	0.137	97	35.0
4.41	(10.0)		5.59	(0.009)	0.132	94	31.0
4.34	(10.5)		6.16	(0.014)	0.127	90	28.0
4.19	(11.0)		6.81	(0.025)	0.116	83	25.5
4.03	(11.5)		7.47	(0.037)	0.104	74	23.0
3.45	(12.0)		8.55	(0.079)	0.062	44	20.5
3.22	(12.5)		9.28	(0.096)	0.045	32	18.5
3.11	(13.0)		9.89	(0.104)	0.037	26	17.5
3.03	(13.5)		10.47	(0.110)	0.031	22	16.5
2.99	(14.0)		11.01	(0.113)	0.028	20	16.0
2.95	(14.5)		11.55	(0.116)	0.025	18	15.0
2.86		(1)	12.64	(0.122)	0.019	13	14.0
2.81		(2)	13.69	(0.126)	0.015	11	13.0
2.75		(4)	15.75	(0.130)	0.011	8	10.2
2.71		(10)	21.79	(0.133)	0.008	6	8.0
2.67		(20)	31.83	(0.136)	0.005	4	5.5
2.63		(50)	62.87	(0.138)	0.003	2	2.8
		(200)	212.00	(0.139)	0.002	1	0.8
		(400)	412.00	(0.140)	0.001	1	0.4
		(1000)	1012.00	(0.141)	0.000	0	0.2
		(2000)	2012.00	(0.141)	0.000	0	
		(5000)	5012.00	(0.141)	0.000	0	

Table 2. Pressure correction for hanging mercury column in penetrometer.

Penetrometer Reading (cm^3)	Pressure Correction (p.s.i.)
0.00	4.53
0.01	4.40
0.02	4.25
0.03	4.15
0.04	4.00
0.05	3.85
0.06	3.75
0.07	3.60
0.08	3.45
0.09	3.30
0.10	3.15
0.11	3.00
0.12	2.85
0.13	2.75
0.14	2.60
0.15	2.45
0.16	2.30
0.17	2.15
0.18	2.00
0.19	1.85
0.20	1.75

pressure in the sample is shown in column (4) of Table 1. The functional pore value is column (6) and is the reciprocal of the penetrometer stem reading. Column (7) is the percent of the total pores remaining unfilled at the absolute pressure recorded in column (4). The pore diameter shown in column (8) is calculated from equation (17) using the absolute pressure value in column (4).

Gamma Beam Attenuation System

For the experimental determination of permeability values flow cells were prepared. To determine the uniformity of packing of these cells, to determine bulk specific gravity, and in non-saturated conditions to determine changes in water content a non-destructive sampling method is required. One such non-destructive sampling method is based on the attenuation of gamma radiation. The method reported by Gurr (1962), Ferguson and Gardner (1962), Rawlins and Gardner (1963), Davidson and Nielsen (1963), and Stammers (1966) was used.

Theory

Beer's law is used to calculate water content and bulk specific gravity with gamma radiation. The attenuation of monoenergetic gamma radiation for a fixed source-detector distance is calculated by

$$I = I_0 e^{-\mu\rho x} \tag{18}$$

where I_0 is the radiation intensity with no interference, I is the attenuated intensity, μ is the attenuation coefficient, ρ is the density, and x is the thickness of the material through which the radiation is passing. Equation (18) is valid if all quanta recorded are of a single energy. This condition was met by collimating the radiation at the source and allowing it to pass through an opening in the shield protecting the detector of the same configuration as the collimator on the source. Discriminator circuitry in the counting equipment was also employed. Thus, only the unscattered radiation which retained its initial energy is recorded.

The use of equation (18) requires the determination of the mass adsorption coefficient, density and thickness of the several materials for the measurement of the water content and bulk density of the porous medium being measured. In terms of these coefficients, equation (18) may be rewritten as

$$I = I_0 e^{-(\mu_s \rho_s + \mu_w \theta) x_s} \quad . \tag{19}$$

Equation (19) must also be written to include the adsorption of gamma photons by the soil container walls. The equation (19), neglecting air may be rewritten as

$$I_M = I_0 e^{-(\mu_s \rho_s + \mu_w \theta) x_s - (\mu_c \rho_c x_c)} . \qquad (20)$$

This equation gives the intensity of the radiation transmitted through a moist porous medium. The corresponding equation for a dry soil is

$$I_D = I_0 e^{-(\mu_s \rho_s x_s - \mu_c \rho_c x_c)} . \qquad (21)$$

Division of equation (20) by equation (21) yields

$$\frac{I_M / I_0}{I_D / I_0} = e^{-\mu_w \theta x_s} \qquad (22)$$

and thus

$$\theta = \frac{\ell n \left(\frac{I_D / I_0}{I_M / I_0} \right)}{\mu_w x_s} \qquad (23)$$

where θ is the volumetric soil water content in percent, μ_w is the adsorption coefficient for water (0.1948 when Am^{241} is used as a gamma source), and x_s is the thickness of the soil sample. To determine the bulk specific gravity, ρ_s, of the porous medium the intensity of the radiation transmitted through the empty container, I_E must be known. The appropriate equation is

$$I_E = I_0 e^{-\mu_c \rho_c x_c} \tag{24}$$

where μ_c is the adsorption coefficient of the container walls, ρ_c is the bulk specific gravity of the container material, and x_c is the wall thickness of the container. Division of equation (21) by equation (24) yields

$$\frac{I_D / I_0}{I_E / I_0} = e^{-\mu_s \rho_s x_s} \tag{25}$$

and thus

$$\rho_s = \frac{\ell_n \dfrac{I_E / I_0}{I_D / I_0}}{\mu_s x_s} \tag{26}$$

where μ_s is the adsorption coefficient of the soil or porous material.

Equipment

The source of low energy gamma radiation employed was 229 millicuries of AM^{241}. Am^{241} has a near monoenergetic gamma output with approximately 60 percent of its radiation having an energy of 0.061 Mev. With the low energy output, a minimum of shielding is required. Furthermore, the optimum sample thickness for this energy is four to five centimeters whereas with the use of Cs^{137}, a frequently used gamma source in gamma attenuation equipment, the

optimum sample thickness is 19 centimeters (Gardner, 1966). Thus, the use of AM^{241} considerably reduces the quantity of porous material and shielding required for water content and bulk specific gravity measurements.

The gamma photons were monitored with a scintillation detector consisting of a sodium iodide, thallium activated crystal three inches in diameter and two inches thick, a photomultiplier tube, and a pre-amplifier. A Hewlett-Packard single channel gamma spectrometer was employed for counting the radiation detected by the scintillation tube. This spectrometer consisted of a high voltage power supply (Model 5551A) for the scintillation tube (Model HP 10602A) and a scaler, timer, and pulse height analyzer (Model HP 5201L). The output from the scaler was digitized and routed directly to a printer (Model HP 562AR). A scintillation count for any preset time was printed. A digital to analog converter (Model HP 580A) was included which allowed a strip chart recording with a Heathkit (Model EUW-20A) recorder when desired. Placing an integrating voltmeter across the output of the digital to analog converter would give the same information as the rate meter described by Stammers (1966). The pulse height analyzer "window" was set to direct transmitted gamma radiation of 0.061 ± 0.015 Mev.

The arrangement of the source and detector is shown in Figure 5. The AM^{241} source holder and the scintillation tube shield

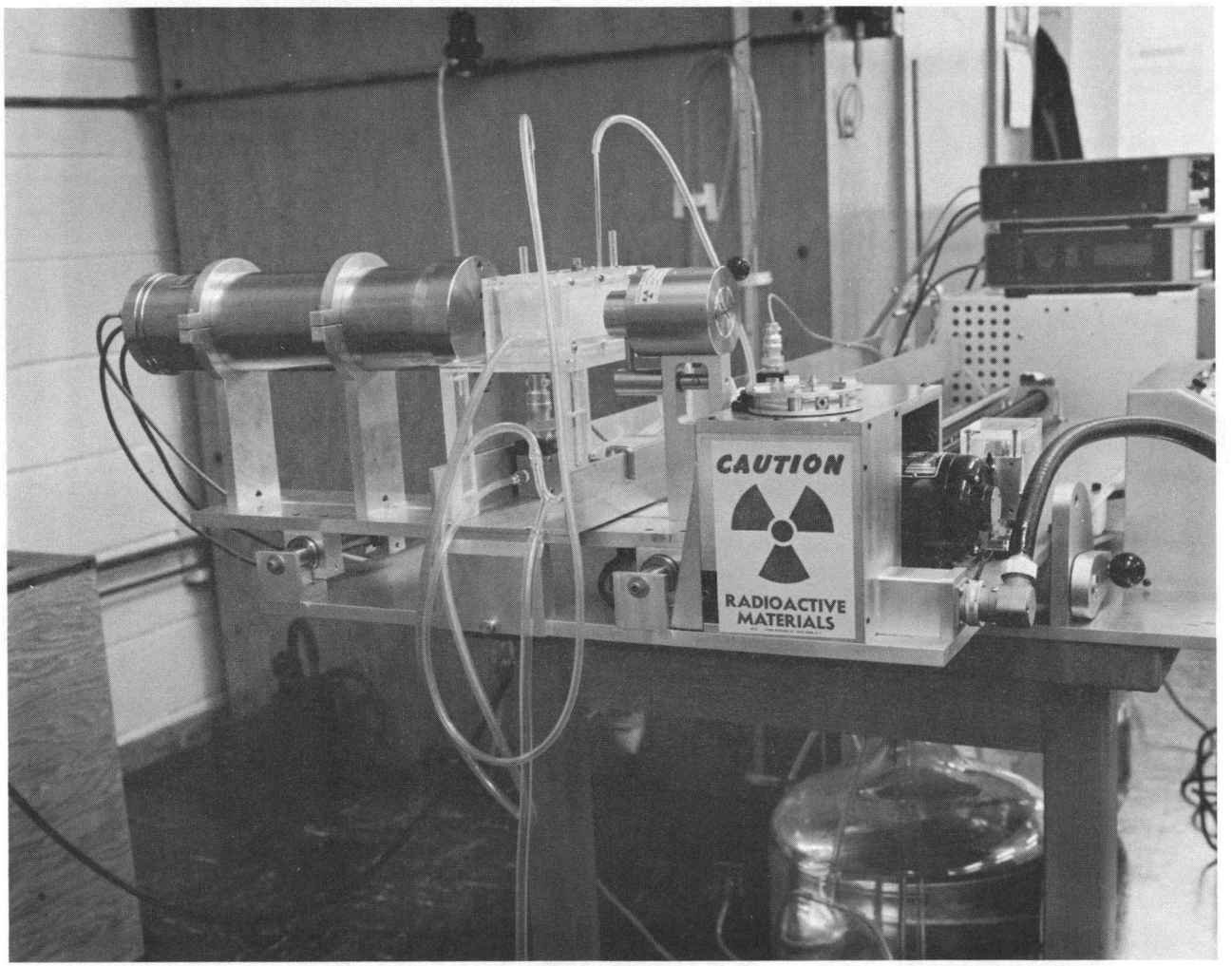

Figure 5. Side view of gamma source container, scintillation detector and flow cell for measuring permeability.

was constructed of one inch thick stainless steel. A tapered collimating slit one centimeter long and one millimeter wide was provided on both the source holder and the scintillation tube shield. The collimating slits were aligned with a mercury vapor light beam. A shield, as shown in Figure 6, was constructed to pass in front of the source collimating window when radiation was not being measured. A one centimeter thick plastic box that could be secured with a lock was placed over the source holder when it was not in use to meet radiation safety requirements.

An automatic tracking system as shown in Figure 6 was constructed to move both the source and the detector past the sample being inspected. Controls were provided for the system to continuously scan the length of the flow column or to stop for a scanning period of from five seconds to six minutes at intervals of 1.0, 1.5, or 2.0 centimeters. A repeat scan system was provided so that the tracking system would move continuously back and forth the present length with a possible cycle delay time up to 30 hours.

In this study a standard scintillation count was always made through a one centimeter aluminum bar immediately before or after the sample density measurement. This insured a correction for any equipment "drift" with time, equipment failure, or change in room temperature.

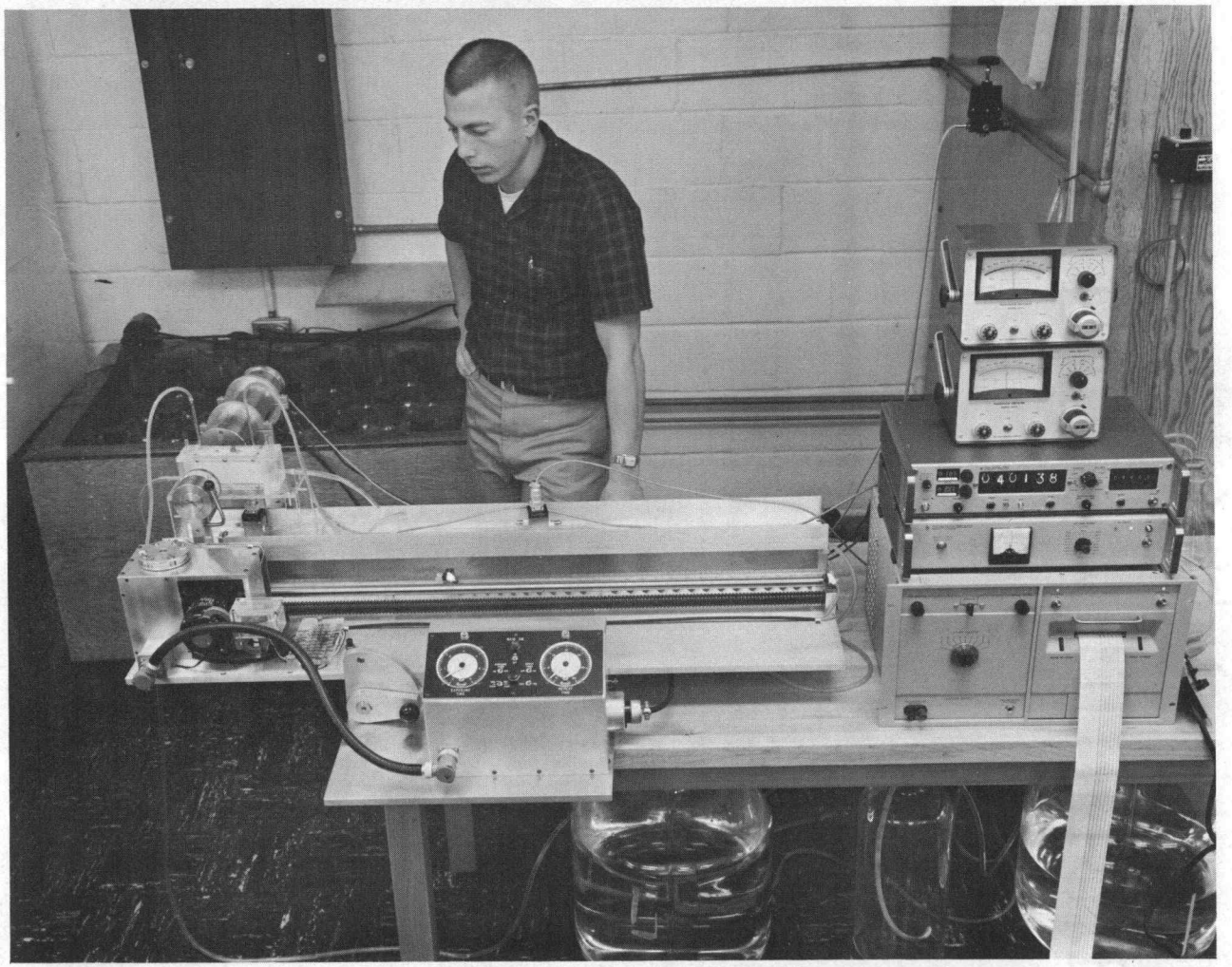

Figure 6. Front view of gamma beam attenuation system and automatic gamma source-detector tracking system.

Flow Cells

Flow cells for measuring permeability, as shown in Figure 7, were constructed of pre-shrunk plastic with an inside cross-section four centimeters high, four centimeters wide, and 16.0 centimeters long. The top and bottom were made of 1.27 centimeters thick plastic and the sides were made of 0.635 centimeter plastic. All pieces were fused together with plastic cement. The square porous plates used were four centimeters on a side and were cut from 2.5 millimeter thick, medium porosity pyrex fritted glass discs. These porous plates have a bubbling pressure of approximately 150 centimeters of water.

An adhesive sealant "silastic 732RTV" produced by Dow Corning was used to seal the porous plates to the end plate and to seal the end plate to the flow cell. This material is very quick drying (approximately one hour) and can be easily cut to disassemble the flow cell for reuse. Two taps were provided to the cavity behind the porous plates so that air could be bled from the system.

Two tensiometers were installed three centimeters from the end plate and ten centimeters apart for the measurement of head loss in the flow column. The tensiometers employed were ten millimeter diameter medium porosity gas dispersion tubes and were installed flush with the inside surface of the top plate of the column. Initially

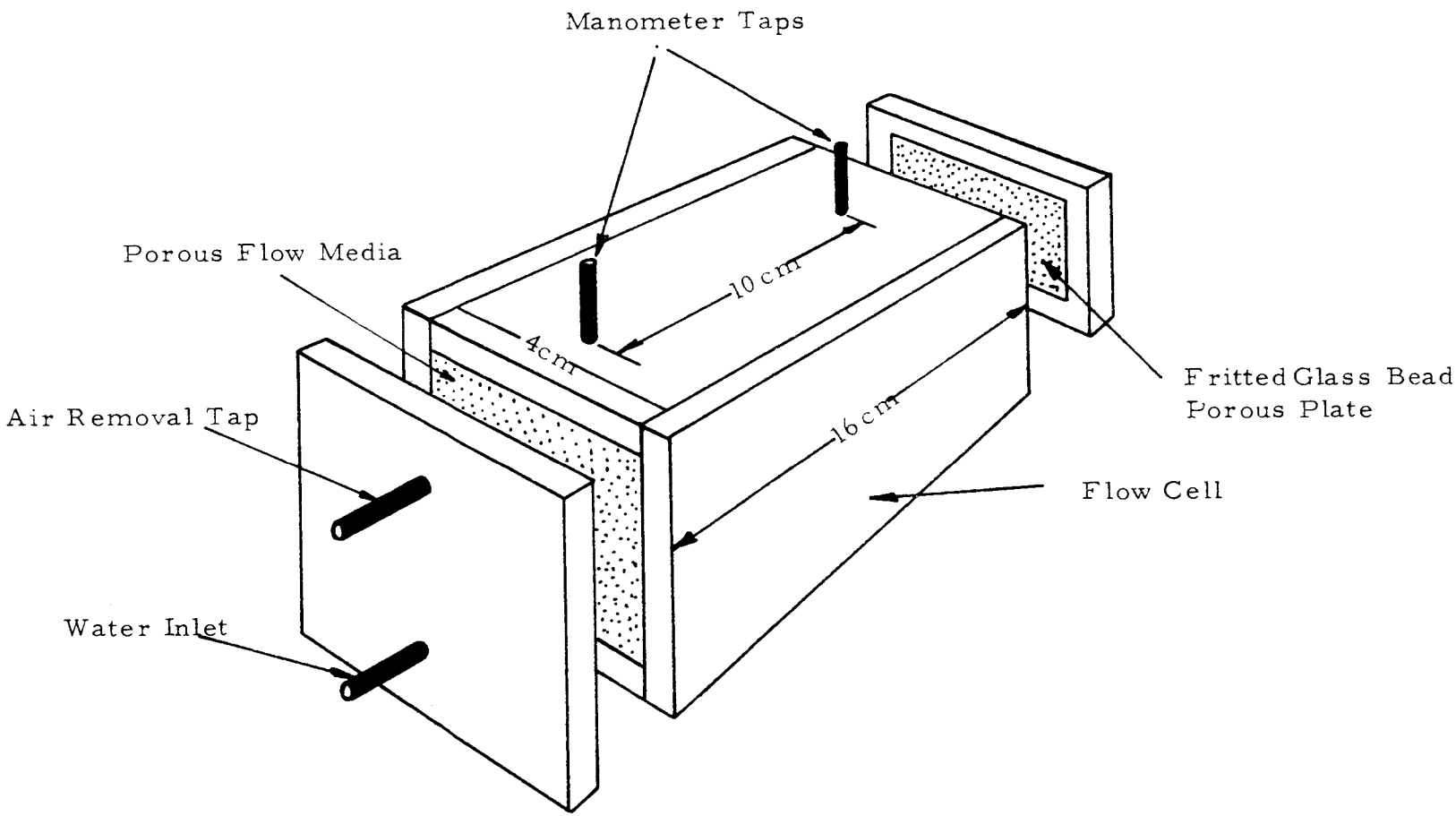

Figure 7. Schematic diagram of plastic flow cell for measuring permeability.

a Pace pressure transducer (Model KP 15) calibrated to measure 0.01 centimeter increments of water pressure was used with a Pace indicator unit (Model CD 25) to measure pressure head at the tensiometers. This instrument was not stable over the period of time necessary for reaching equilibrium conditions. Thus, water manometers were employed with the tensiometers. The pressure transducer was used as a "differential manometer" across the two tensiometers to show when the flow system reached a steady state condition. With the small cross sectional area of the porous plate in the tensiometer and the very small pores, clogging of these pores frequently occurred. This condition occasionally caused a "lag" in the manometer readings. To eliminate this problem, distilled water was flushed in reverse through the tensiometer after each use of the flow cell. A schematic drawing of the cross-section of the end plate and tensiometer is shown in Figure 8.

The source of water for the flow cell was from a five liter "mariotte" bottle. Water flowing through the cell was released into a collection bottle at a point having positive head with respect to the flow cell location. The flow velocity through the cell was measured at the outlet. The diagram of the flow system is shown in Figure 9.

Porous Materials Tested

Over a period of time several equations have been proposed

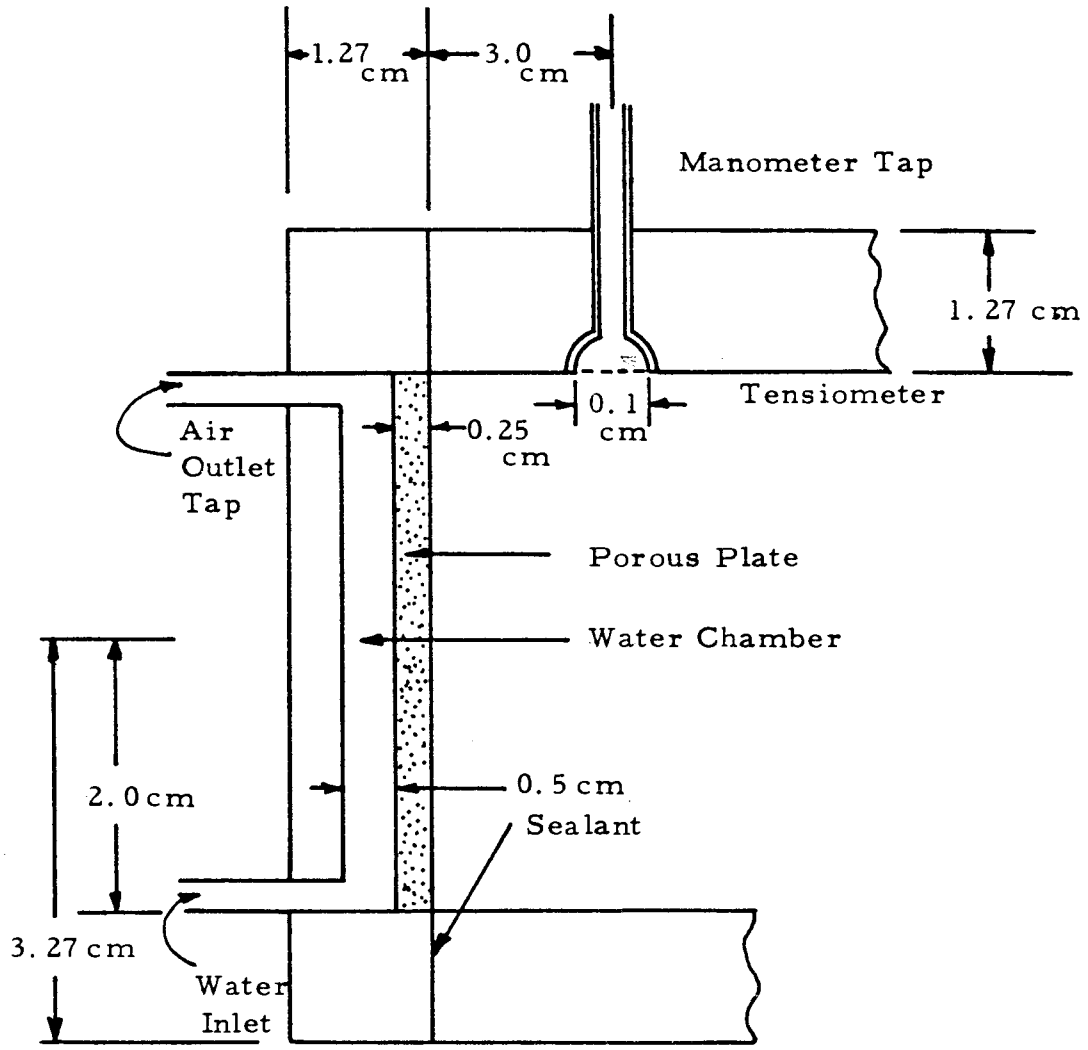

Figure 8. Schematic diagram of the cross-section through the porous end plate and tensiometer.

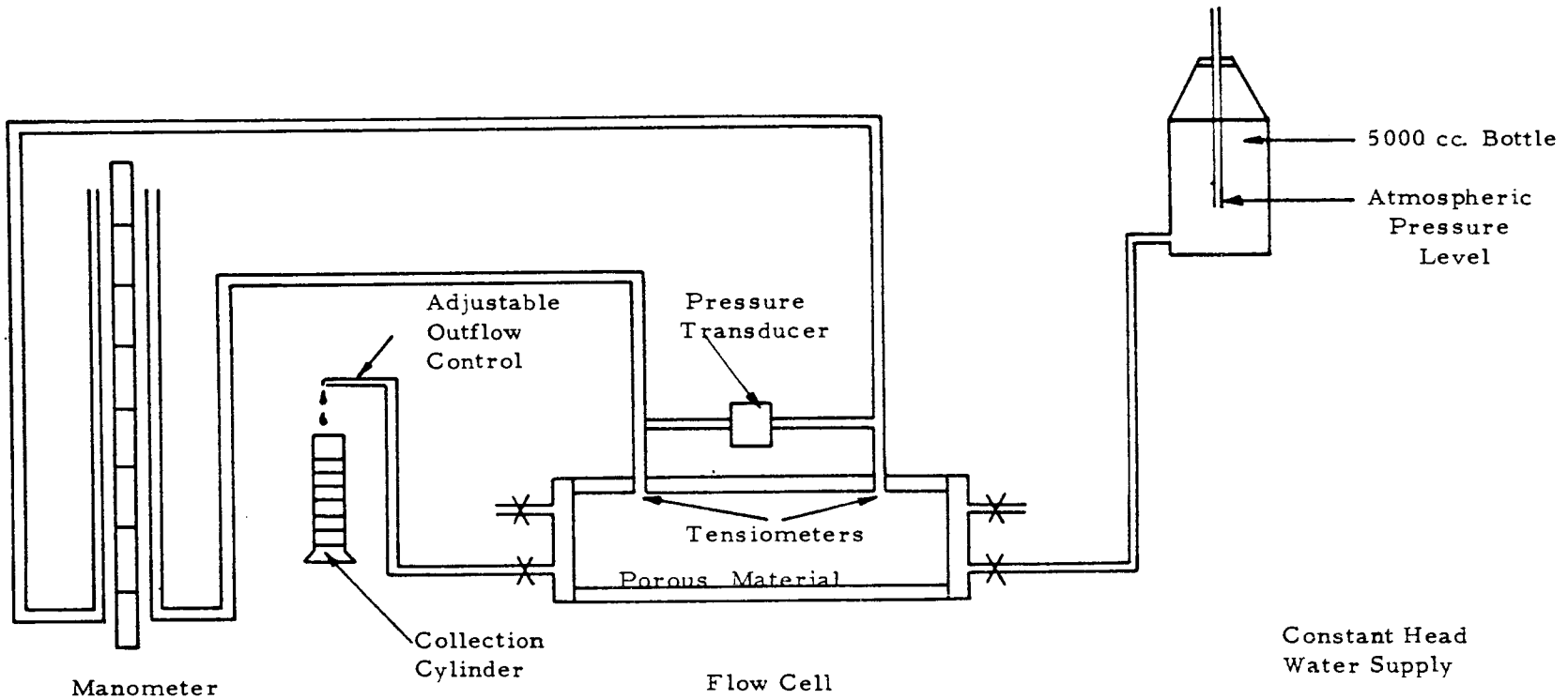

Figure 9. Schematic diagram showing manometers, flow cell, and constant head water supply.

by which the permeability of a porous medium can be predicted from pore size distributions. The research reported in this dissertation is based on the premise that only through a series of systematic experiments the apparent disagreement between the several methods can be resolved. For this reason a series of porous materials of predetermined size distributions were prepared.

Glass beads (3M "Superbrite") and crushed quartz sand were used as the material from which the porous media were prepared. The glass beads and the quartz sand were separated into predetermined size classes by sieving. The selected sieve size classes are shown in Table 3. Materials in the different sieve size classes were then mixed in predetermined ratios. The mixing ratios are also shown in Table 3.

The glass beads have an average bulk specific gravity of 1.53 grams per cubic centimeter and a particle density of 2.45 grams per cubic centimeter. This indicates an average porosity of 37 percent which was also measured by the gamma attentuation system.

The crushed quartz sand was used to obtain a more realistic appraisal of conditions in soils than is possible with the use of glass beads. The beads have smooth spherical surfaces whereas the quartz sand consists of irregular broken crystals containing sharp edges.

Table 3. Permeability size class designations.

Classes		Percent Sieved Size Fractions									
Glass Beads	Quartz	208-246	175-208	147-175	124-147	104-124	88-104	74-88	61-74	53-61	44-53
208-246 μ		100									
1	101	90	10								
2	102	70	10	10	10						
3	103	50	10	10	10	10	10				
4	104	30	10	10	10	10	10	10	10		
5	105	10	10	10	10	10	10	10	10	10	10
175-208 μ			100								
6			90	10							
7	107		60	10	10	10	10				
8	108		40	10	10	10	10	10	10		
9	109		20	10	10	10	10	10	10	10	10
147-175 μ				100							
10	110			90	10						
11	111			70	10	10	10				
12	112			50	10	10	10	10	10		
13	113			30	10	10	10	10	10	10	10
124-147 μ					100						
14					90						
15	115				60	10	10	10	10		
16					40	10	10	10	10	10	10
104-124 μ						100					
17						90	10				
18	118					70	10	10	10		
19	119					50	10	10	10	10	10
88-104 μ							100				
20							90	10			
21	121						60	10	10	10	10
74-88μ								100			
22								90	10		
23	123							70	10	10	10
61-74 μ									100		
24									90	10	
25	125								80	10	10
53-61 μ										100	
26										90	10
44-53 μ											100

Experimental Procedure

Each established permeability class was prepared and poured into a flow cell to which one end plate was attached. An extension was fitted to the top of the flow cell and the porous material was poured into the cell through a funnel. The material was filled to a length at least five centimeters longer than the flow cell. After filling the flow cell and its extension, both were vibrated with a hand held, jewelry engraver. This packing motion was continued until no further downward movement from consolidation was observed. This required two to three minutes. The cell extension was removed, the porous material above the end of the cell leveled, and the end plate attached with the sealant.

After the sealant was dry, the flow cell was placed in the gamma attenuation system and the dry bulk specific gravity as determined by equation (26), was measured at one centimeter increments along the length of the column. If a variation in bulk specific gravity variation greater than five percent was recorded, the sample was repacked.

If the flow cell's packing was acceptable, it was placed in a small vacuum chamber constructed of acrylic plastic. In the chamber the flow cell was attached to a source of distilled water. After the vacuum chamber had been evacuated, the distilled water was

released into the flow column to saturate the sample. This procedure was established to remove possible flow resistance due to entrapped air in the sample material within the flow cell. Once the sample was saturated, it was placed in the gamma attenuation system and the tensiometers connected to the manometers and the pressure transducer. When a steady state flow condition was indicated by the pressure transducer, the flow rate, water temperature and head differential were measured. Also, the saturated bulk specific gravity was measured with the gamma attenuation system to record the saturated porosity. This measurement insured that the sample was saturated and simplified the calculation of the saturated porosity required for establishing calculated permeabilities. Identical equipment was constructed to measure the flow rate on two cells simultaneously.

After the permeability was measured a sample of porous material was removed from the flow cell and a pore size distribution curve for the sample was measured with the mercury intrusion porosimeter.

RESULTS

Porosimeter Data

Pore aperture size distribution curves obtained with the mercury intrusion porosimeter for all 54 size classes of glass beads and crushed quartz sand are shown in the Appendix. These curves were constructed from the data recorded and calculated in the manner shown in Table 1. The curves shown in the Appendix are plotted as accumulation curves. In Figure 10 pore size frequency distributions of three sieve size classes of glass beads and quartz sand are compared. The frequency distribution curves show that the quartz sand has a mean pore aperture radius several microns smaller than glass beads with the same distribution of particle sizes.

Experimental Permeability Data

Permeability measurements were made on all size classes of glass beads with the results shown in Table 5, column (6). The measured permeabilities for the crushed quartz sand classes are shown in Table 6, column (6).

Calculated Permeability Data

Several investigators (Purcell, 1949; Childs and Collis-George,

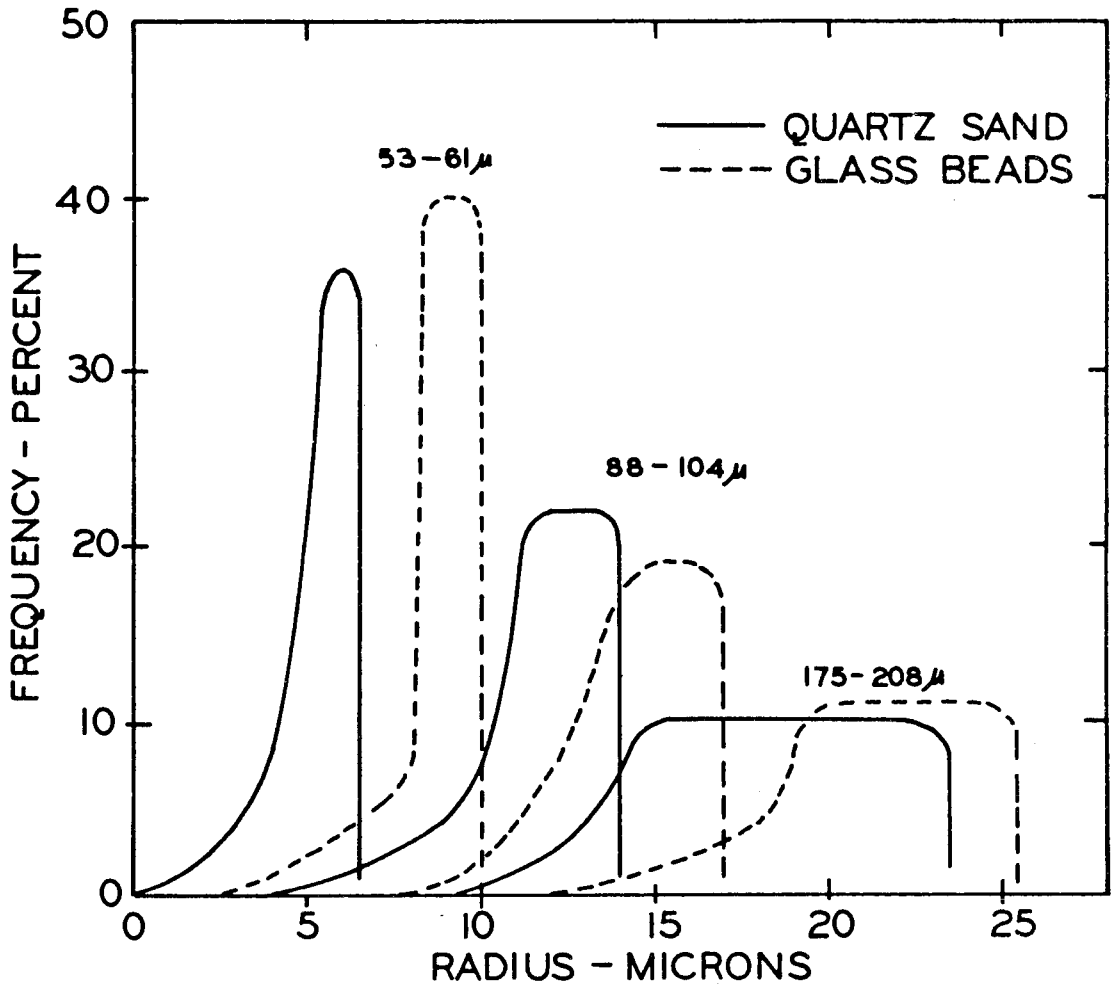

Figure 10. Pore radius frequency distributions for three sieve sizes of glass beads and quartz sand.

1950; Marshall, 1958; and Laliberte, 1966) have proposed methods of calculating saturated intrinsic permeability from pore size distribution data. The equation of Marshall (equation 13) was chosen as the most practical equation to use with the information obtained from the porosimeter.

Calculation of the Permeability

In order to calculate the intrinsic permeability the pore size distributions were divided into ten divisions. In each division a mean pore radius was determined. An example of the calculations required to calculate the permeability is shown in Table 4. The calculated permeabilities of all size classes of glass beads and quartz sand are shown in column (5) of Table 5 and Table 6 respectively.

In Tables 5 and 6 the calculated pore radii sum of squares, column (2), the mean pore radius, column (3), and the saturated porosity as measured by the gamma attenuation system, column (4), for the designated size classes are shown.

Table 4. An example of the procedures used in calculating the sum of the pore radii squared term in equation (13).

Test material: Glass bead size class 147-175μ.

Equation: $\Sigma r_n^2 = [\, r_1^2 + 3r_2^2 + 5r_3^2 + \cdots + (2n-1)r_n^2 \,]$

n = number of fractions or divisions or total pore volume (10).

r = mean pore radius in each of n equal fractions in decreasing order of size.

"n" fraction	Pore volume %	Radius	Radius squared μ^2	Constant	Product μ^2
r_1	95	22.30	497.29	1	497
r_2	85	21.70	470.89	3	1413
r_3	75	20.90	436.81	5	2184
r_4	65	20.25	410.06	7	2870
r_5	55	19.50	380.25	9	3422
r_6	45	18.75	351.56	11	3867
r_7	35	18.10	327.61	13	4259
r_8	25	17.30	299.29	15	4489
r_9	15	13.00	169.00	17	4684
r_{10}	5	10.00	100.00	19	3311
					$\Sigma r^2 = 30996$

Table 5. Glass bead calculated and measured permeabilities.

1 Particle Size Class	2 Sum of Radii Squared μ^2	3 Mean Pore Radius μ	4 Saturated Porosity %	5 Calculated Permeability μ^2	6 Measured Permeability μ^2	7 Adjusted Sum of Radii Squared μ^2	8 Adjusted Calculated Permeability μ^2
208-246μ	50,539	24.9	37	8.65	39.10	217,163	37.16
1	42,721	22.8	38	7.71	34.44	179,784	32.45
2	33,698	20.4	38	6.08	29.90	139,194	25.12
3	25,004	17.4	36	4.05	18.94	98,620	15.98
4	15,828	13.8	34	2.29	7.63	58,664	8.48
5	8,252	9.9	34	1.19	4.52	28,043	4.05
175-208 μ	43,558	24.2	37	7.45	32.09	183,434	31.39
6	40,979	22.8	36	6.64	25.96	180,043	29.17
7	26,688	17.9	36	4.32	23.21	106,369	17.23
8	15,000	13.4	34	2.17	8.95	55,180	7.97
9	7,630	9.6	32	0.98	4.26	25,664	3.28
147-175 μ	30,996	19.4	37	5.30	21.07	125,169	26.70
10	24,496	17.3	37	4.19	17.80	97,573	21.42
11	20,607	15.8	37	3.53	11.84	79,381	13.58
12	18,648	15.0	37	3.19	10.92	70,880	12.13
13	7,389	9.5	34	1.07	4.86	24,661	3.56
124-147μ	25,360	17.4	37	4.34	17.68	100,205	17.15
14	22,351	16.5	37	3.82	14.03	86,853	14.86
15	16,890	14.2	36	2.74	10.24	63,351	10.26
16	7,928	9.6	35	1.21	5.13	26,817	4.11
104-124 μ	18,692	15.0	37	3.20	9.34	70,897	12.13
17	16,681	14.2	37	2.85	12.62	60,089	10.62
18	13,988	12.9	36	2.27	8.65	50,835	8.24
19	8,513	10.2	35	1.30	4.93	29,136	4.46
88-104μ	13,176	12.5	37	2.25	6.97	47,380	8.11
20	10,939	11.4	37	1.87	6.84	38,353	6.56
21	8,215	9.9	37	1.41	3.77	27,752	4.75
74-88μ	10,084	11.1	37	1.73	5.75	34,879	5.97
22	7,179	9.8	38	1.41	6.25	26,480	4.78
23	7,473	10.1	36	1.21	4.18	24,947	4.04
61-74μ	8,274	10.0	37	1.42	4.82	27,917	4.78
24	6,966	9.1	37	1.19	4.43	22,978	3.93
25	6,734	8.8	36	1.09	5.16	22,137	3.58
53-61 μ	7,294	9.9	37	1.25	3.89	24,227	4.14
26	5,198	8.8	37	0.89	3.12	16,489	2.82

Table 6. Quartz sand calculated and measured permeabilities.

1 Particle Size Class	2 Sum of Radii Squared μ^2	3 Mean Pore Radius μ	4 Saturated Porosity %	5 Calculated Permeability μ^2	6 Measured Permeability μ^2	7 Adjusted Sum of Radii Squared μ^2	8 Adjusted Calculated Permeability μ^2
208-246μ	41,029	24.3	45	10.38	69.58	186,739	47.27
101	38,739	23.5	46	10.24	67.78	164,059	43.39
102	25,527	19.2	44	6.17	26.14	101,858	24.65
103	14,350	12.1	42	3.16	14.85	50,347	11.10
104	7,712	10.5	40	1.54	4.75	22,712	4.54
105	4,987	8.7	38	0.90	3.93	13,313	2.40
175-208 μ	28,101	19.8	46	7.43	25.98	110,561	29.32
107	14,225	14.2	42	3.13	5.61	49,237	10.86
108	7,950	10.8	37	1.36	3.78	21,046	3.60
109	4,701	8.3	37	0.80	2.48	12,402	2.12
147-175 μ	23,648	18.2	47	6.53	19.90	88,921	24.55
110	18,800	15.7	48	5.41	12.57	67,550	19.45
111	11,792	13.1	47	3.26	9.23	39,630	10.94
112	8,549	11.2	44	2.07	7.13	25,828	6.25
113	5,124	8.7	43	1.18	2.18	13,871	3.206
124-147 μ	12,636	13.5	48	3.64	13.68	43,436	12.51
115	7,815	10.7	43	1.81	4.44	23,114	5.34
104-124	10,262	11.5	48	2.96	8.55	32,487	9.36
118	6,958	12.6	49	2.09	7.74	20,001	6.06
119	4,909	10.1	46	1.30	4.80	12,911	3.41
88-104 μ	6,871	9.9	48	1.98	5.36	20,830	6.00
121	4,900	10.0	46	1.30	3.44	12,909	3.41
74-88 μ	5,375	9.1	49	1.61	4.21	14,367	4.31
123	4,155	8.0	45	1.05	1.86	10,511	2.66
61-74 μ	3,471	7.2	50	1.08	2.45	8,282	2.59
125	3,180	6.4	50	0.99	2.11	7,403	2.31
53-61 μ	2,436	6.1	51	0.79	2.06	5,211	1.694
44-53 μ	1,787	5.3	51	0.58	1.51	3,523	1.145

DISCUSSION

It is quite apparent from colums (5) and (6) of Tables 5 and 6 that there is a considerable disagreement between the measured permeabilities and those calculated by Marshall's equation from porosimeter data. This disagreement can result from either an error in the measurement of the saturated porosity or an incorrect evaluation of the pore aperture size distribution. A check on the procedure for measuring the saturated porosity with the gamma ray system shows that these measurements were not a source of error.

In Figure 11 the measured permeabilities of glass beads are plotted as a function of the sum of pore aperture radii squared to test the influence of the pore radii on the intrinsic permeability. The same procedure was followed in Figure 12 for the quartz sand size classes. Both figures show that the intrinsic permeability is a direct function of the pore aperture radius. Thus, it must be concluded that the magnitude of the pore radius functional term is in error. It should be noted here that all modifications of Marshall's equation (Millington and Quirk, 1959, and Jackson, Reginato, and van Bavel, 1965) have been concerned with the porosity function and no one has questioned the validity of the sum of pore radii squared term.

The magnitude of the error described can be measured by finding the ratio between the measured and calculated permeabilities

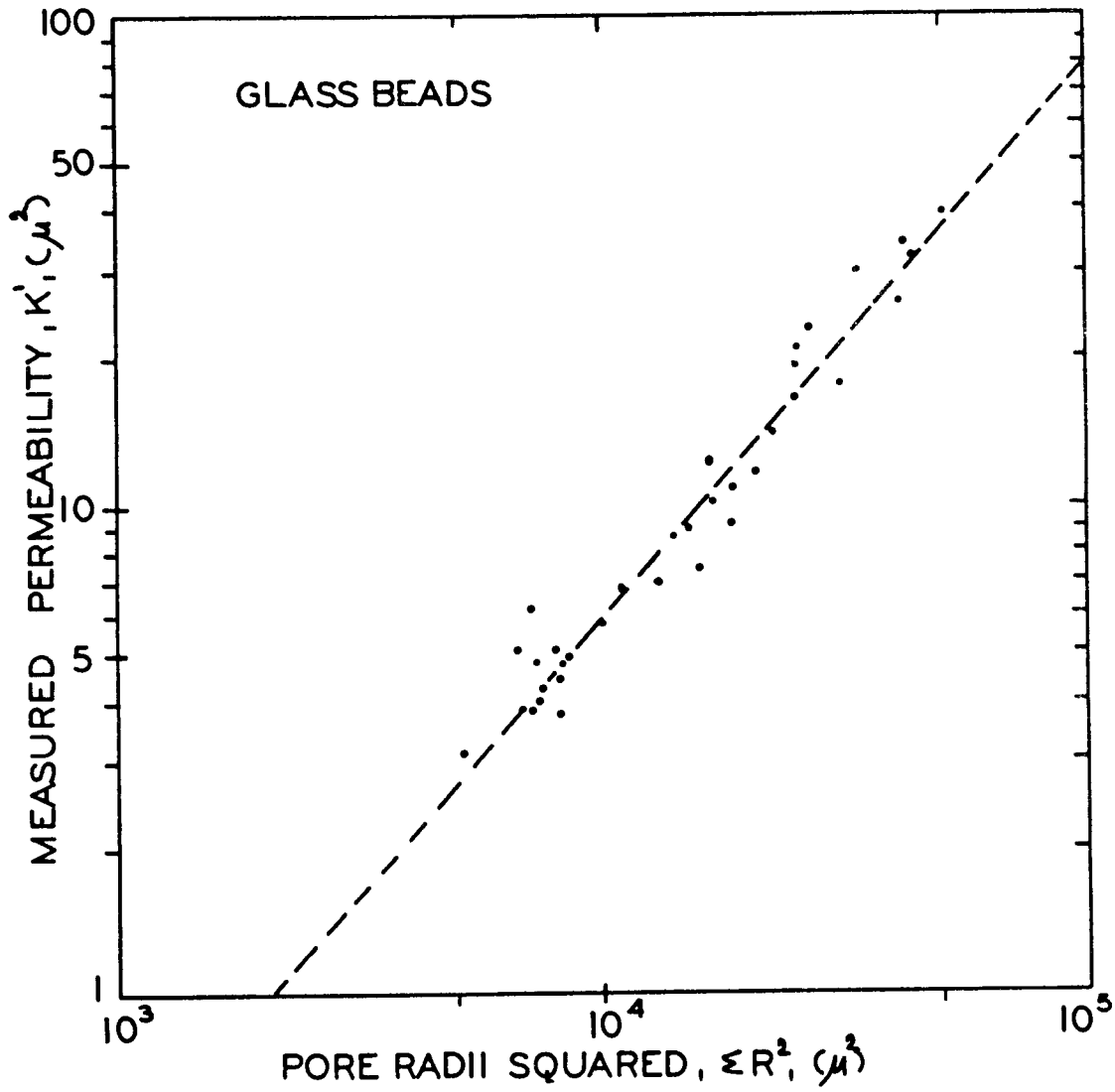

Figure 11. Measured permeability for 35 size classes of glass beads as a function of the sum of the pore radii squared.

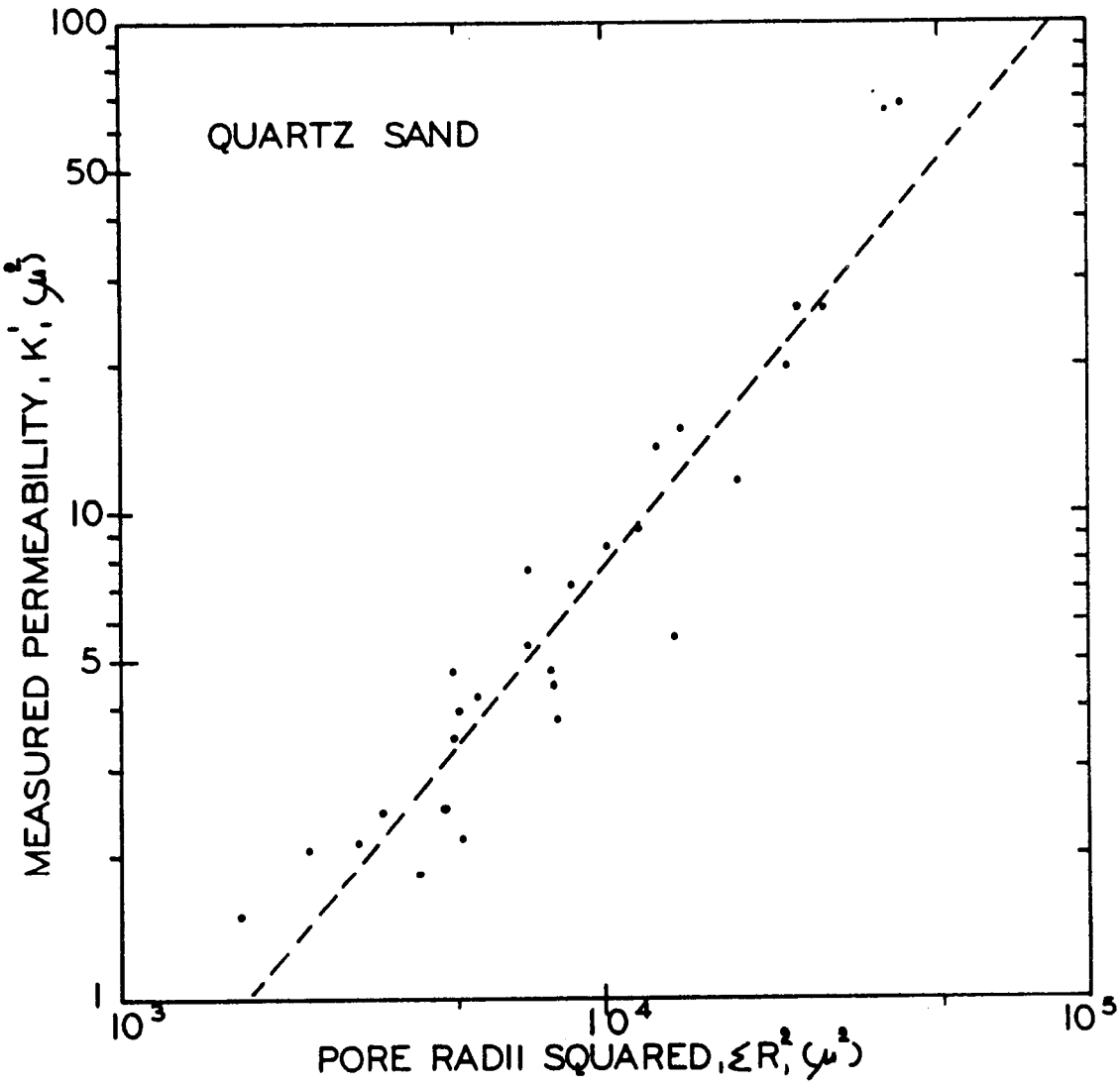

Figure 12. Measured permeability for 28 size classes of quartz sand as a function of the sum of the pore radii squared.

for all classes. This ratio is approximately four with a ratio greater than four for size classes with large sum of pore aperture radii squared values and less than four at smaller values. Thus, it appears that the pore aperture radius as determined by the porosimeter is less than the effective radius, and that the ratio of the measured and effective radius is systematically greater from smaller to larger pores.

To evaluate this apparent systematic error, the mean pore radius for all classes were plotted as a function of the sum of the pore aperture radii squared term used in Marshall's equation. The regressions for both glass beads and quartz sand are shown in Figure 13. By use of these regressions the square root of the ratio between measured and calculated permeability can be plotted as a function of the pore radius. These plots are shown in Figure 14. The regression equation for glass beads is

$$Y = 1.26 + 0.6015 \log X$$

and for the quartz sand

$$Y = 0.73 + 1.0124 \log X.$$

Figure 14 shows that the pore radius required to calculate permeabilities to match the experimental permeabilities needs to be multiplied by a factor of two at a pore radius near 20 microns. For pores

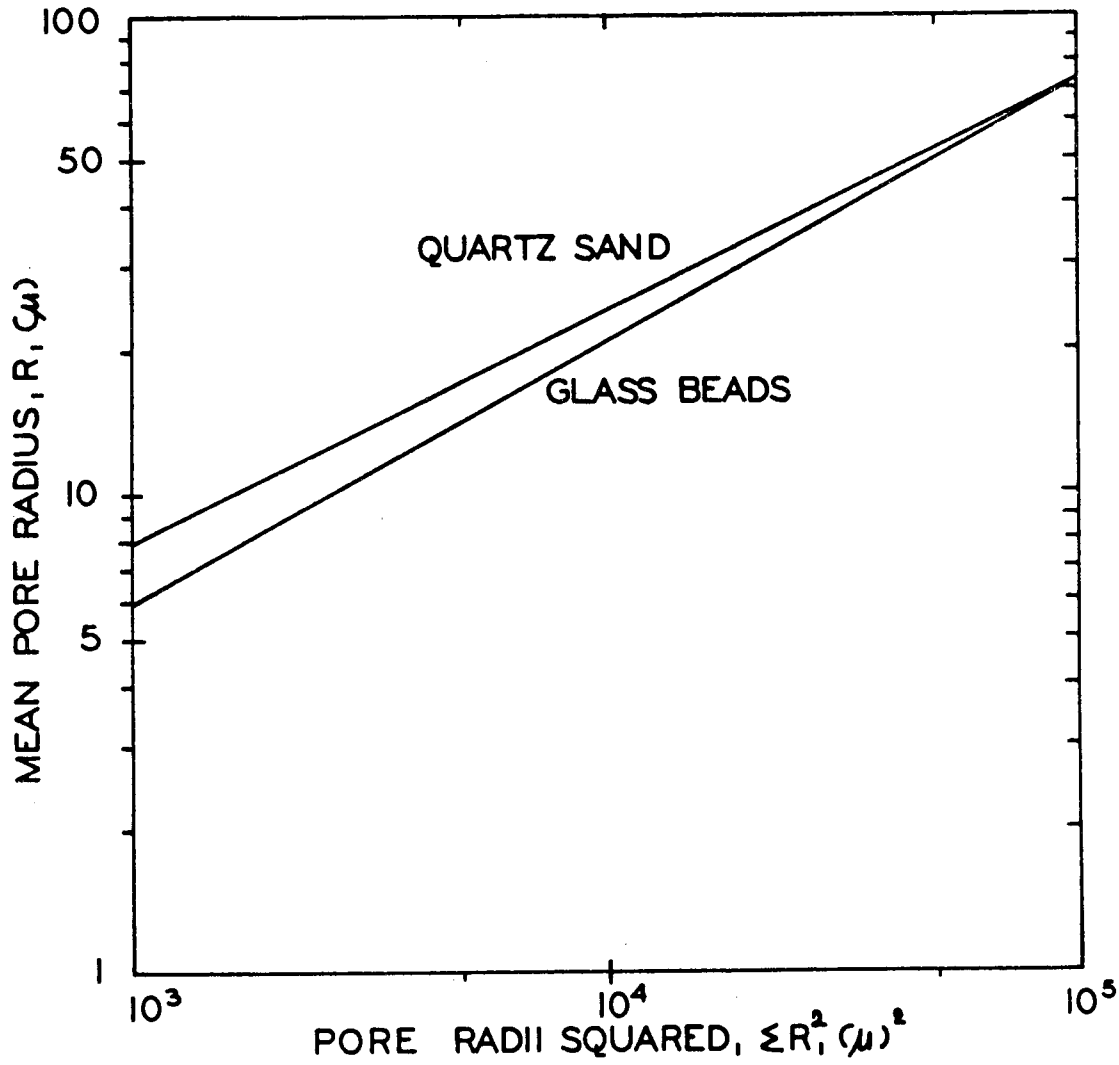

Figure 13. Correlation between the mean pore aperture radius and the sum of the pore radii squared for glass beads and quartz sand.

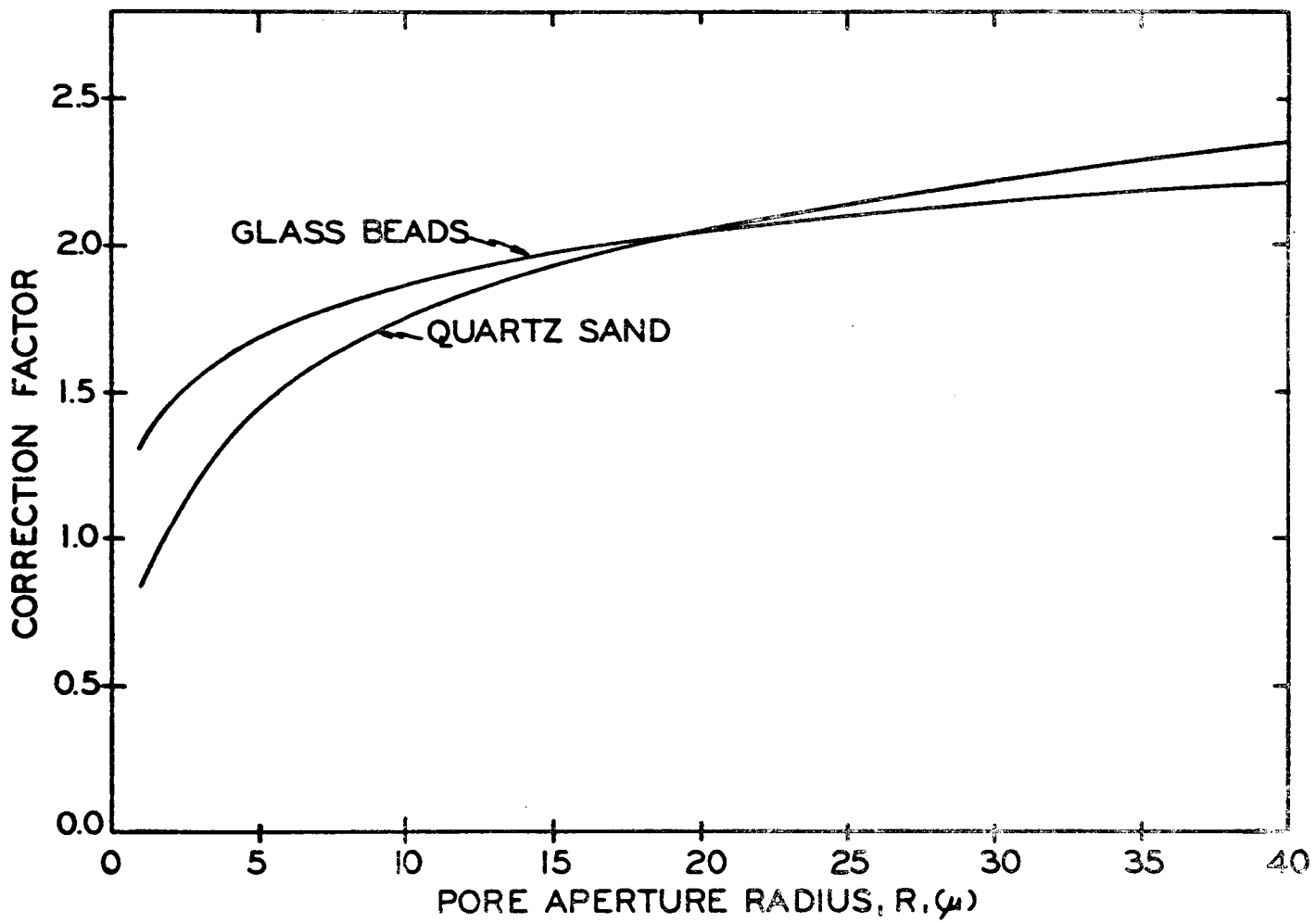

Figure 14. The correction factor (square root of the ratio of measured to calculated permeability) as a function of the pore radius.

less than 20 microns the factor becomes less than two and for larger pores the factor is greater than two.

By using the appropriate correction factor regression equation for both glass beads and quartz sand with the pore aperture radii as measured by the porosimeter, a new accumulative pore aperture distribution curve can be constructed. For all size classes these adjusted curves were used to calculate an adjusted pore radii sum of squares. The values obtained are shown in column (7) of Tables 5 and 6. The Marshall equation was used once again to calculate an adjusted permeability. The adjusted calculated permeabilities for all size classes of glass beads and quartz sand are shown in column (8) of Tables 5 and 6. The correlation between the adjusted calculated permeability and the measured permeability is shown in Figure 15 for the glass beads and in Figure 16 for the quartz sand. The regression line shown in both Figures 15 and 16 is for a one-to-one ratio between measured and calculated permeability. Thus, it can be assumed the error in the original calculated permeabilities was in the pore radius size evaluation, and that this was a systematic error depending upon the magnitude of the pore aperture radius.

A different correction factor has been presented for glass beads and for quartz sand. The glass beads have a very smooth surface and the crushed quartz has an extremely rough and sharp surface. Soil would be expected to have a correction factor lying

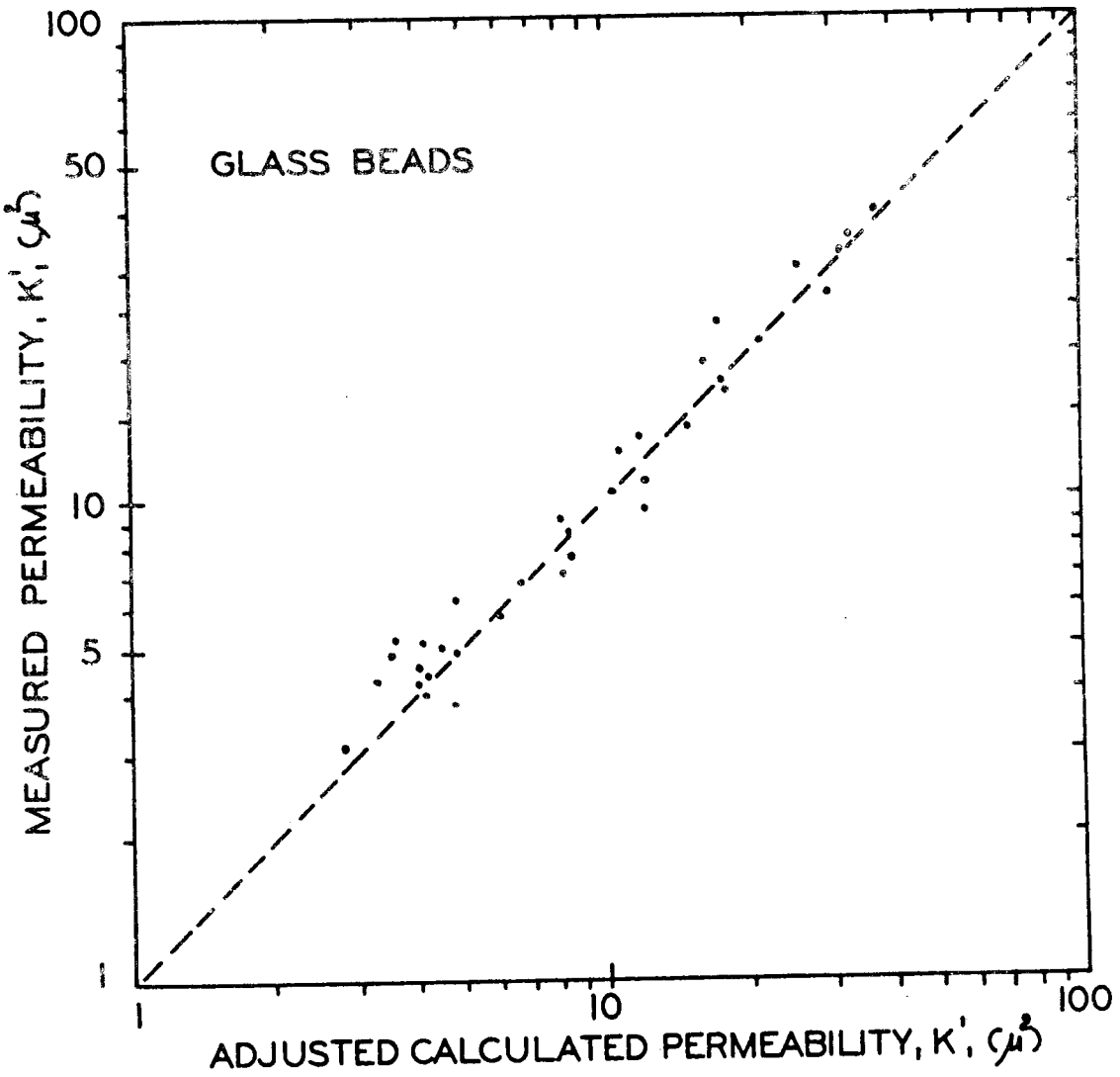

Figure 15. Correlation between measured and adjusted calculated permeability for 35 size classes of glass beads.

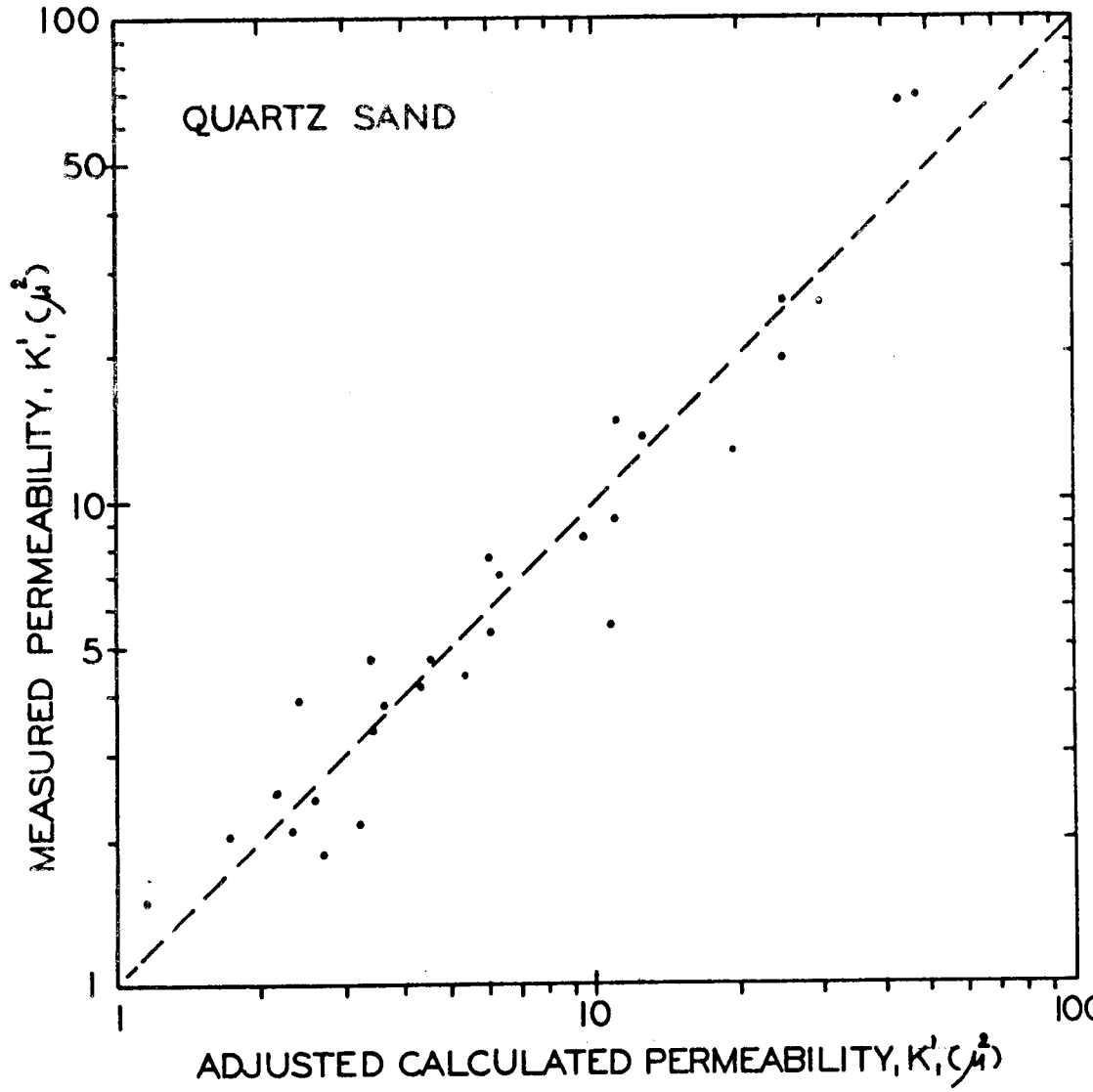

Figure 16. Correlation between measured and adjusted calculated permeability for 28 size classes of quartz sand.

somewhat intermediate.

The question now arises whether this adjustment represents a correction of Marshall's equation or a correction of the equation by which the pore radii were calculated from the porosimeter data. Marshall (1958) noted that his equation is only applicable where the material has no lengthy conducting channels. This occurs where large pores are present in the medium.

This explanation does not appear to be a reasonable one in our case. It does not explain the overestimation of pore sizes below 40 microns. Furthermore, a break down of the Marshall equation should not be expected to occur at the relatively small pore aperture radius of 50 microns.

Consideration of the validity of the pressure of displacement equation (equation 1) used with the porosimeter data holds more promise. In the pressure of displacement equation three variables - pressure, contact angle, and surface tension of the liquid - are present along with one constant, the value two. The pressure applied is quite easily and accurately measured. Both the contact angle and the surface tension of mercury have been thoroughly investigated and given in handbooks (Weast, 1964). Neither term would be expected to change with pressure in the range which it was subjected under this study, and both the contact angle and the surface tension are a property of the liquid. The only intrinsic term involved is the

constant. The constant's value of two is developed from the geometry of a capillary tube with one radius of curvature. Use of this equation for measuring pore aperture sizes of porous materials assumes that the connecting pores have the same geometry as capillary tubes. In soil this is certainly not the case. It is quite possible that the pore shape factor must be considered in an evaluation of the constant and consequently, the size of the pore aperture. Under these considerations, the correction factor used with a porosimeter measured pore aperture radius gives an apparent hydraulic pore aperture radius. This approach would concur with the discussion by Brooks and Corey (1964) on the theoretical basis for the Burdine equation.

It might be noted here that the correction factor value for a small pore radius is less for crushed quartz sand than for glass beads. This means that a given pore size of glass beads would have a higher permeability than for an equal pore size of quartz sand. The pore shape factor is the only conceivable difference in the two pores.

The adjustment can also arise due to a difference in packing of the unconsolidated materials in the porosimeter and that in the flow cells. No real accurate measurement of the bulk specific gravity can be measured in the porosimeter. Under the influence of an initial vacuum and then the subsequent contact with mercury under pressure the sample may have a greater bulk specific gravity than could be

achieved by the packing method used on the material in the flow cells. The bulk specific gravity of the samples placed in the porosimeter were very near those achieved in packing the flow cells. This is certainly a possible source of error, but it is not of the magnitude that must be considered.

The correction factor as a function of pore aperture radius that has been presented, should only be used with the mercury intrusion method. Purcell (1949) has shown that capillary pressure desaturation curves obtained with mercury are not the same as those obtained with water. The consequent pore aperture radius was found to be smaller when measured with mercury than when it was measured using water as the wetting liquid. In Rose's evaluation of Purcell's (Purcell, 1949) article he noted the difference in capillary pressure desaturation curves of mercury and water on the same porous material. His conclusion was that the reservoir liquid used in measuring these curves must be the same as that for which the permeability is tested when comparing the calculated and measured permeabilities. If this is a true statement, the work of Brooks and Corey (1964) and Laliberte (1966) and others who have used soltrol as a liquid in determining capillary pressure desaturation curves is invalid. This is doubtful. It must be considered that permeability is an intrinsic property and should not be concerned with the liquid involved.

The pore aperture size distribution of several size classes of both glass beads and quartz sand were measured with both water and

mercury. The mean measured pore radius as measured by water was always found to be larger than that measured by mercury on both the glass beads and the quartz sand.

Three factors may enter into the reason why capillary pressure desaturation curves are different when measured with mercury and water. First, air is the wetting fluid in the case with the mercury intrusion method. When measuring pore size distributions with water, air is the non-wetting fluid. It is quite possible that air may be adsorbed on the particle until extremely low pressures are reached. This different property of air could alter the dimension of the pore measured by the two techniques.

The influence of packing can be the second important factor. With mercury a dry material is used and the point of complete primary consolidation has been reached before the pore aperture size distribution is measured. To measure the pore aperture size distribution on the drainage phase of the hysteresis cycle of an unconfined sample with water, the porous material must be completely saturated at the beginning of the test. As water is removed by the application of pressure, the process of primary consolidation continues until the sample is completely desaturated. In this process the distribution of pore aperture radii would change with the change in degree of saturation causing an incorrect evaluation of the pore aperture size distribution required for permeability prediction

calculations. If the pore aperture size distribution is measured with water on a confined sample that was packed in the absence of water, or previously consolidated, the correction factor for the effective hydraulic pore aperture radius should be closer to that used with mercury.

The third factor contributing to this difference in pore aperture size distributions may be that water is a polar compound as compared with mercury which is not, and is adsorbed by the surface of solid particles. Thus, a physical-chemical interaction may occur. If this interaction does occur, water can not be used to measure a true intrinsic property of a porous medium.

From these observations the pore aperture radius as measured by mercury is a true evaluation of the physical radius of the pore apertures in the porous material. The systematic correction factor as presented by this dissertation is used to define the effective hydraulic pore aperture radius.

Researcher's disagreement on the correct procedure to predict saturated permeability may have contributed to the incorrect evaluation of the pore aperture size distribution and its effect on permeability. Now, with a reliable method to predict saturated permeability, the prediction of permeabilities at capillary pressures corresponding to conditions less than saturation may be evaluated. Parameters such as bubbling pressure and pore size distribution

index whose values are needed for proposed methods of predicting unsaturated soil water movement may be effectively measured by the mercury intrusion porosimeter.

SUMMARY AND CONCLUSION

A relatively quick and easy method is desirable to measure pore aperture size distributions in porous materials such as soil. The use of a commercial type porosimeter employing the mercury intrusion method has been evaluated for this purpose. Fifty-four different size fractions of glass beads and quartz sand chosen to give a systematic range of pore sizes were tested. Although the sample size is quite limited with the porosimeter, this method does give good reproducible pore aperture size distributions. Both the glass beads and the quartz material used as test materials are considered inert and no evaluation was made of the physical-chemical interactions that may occur between mercury and clay.

Several authors have attempted to use pore aperture size distributions for the prediction of permeabilities. Permeabilities were determined for all 54 size classes of glass beads and quartz sand for which the pore aperture size distributions were measured. The measured permeabilities are compared with the predicted values determined by the Marshall equation (1958). There was a considerable disagreement between the measured and calculated permeabilities. The calculated values were approximately one-fourth the measured values. A good relationship was established between the sum of the pore aperture radii squared as measured by the

porosimeter and the measured permeabilities. The evaluation of the magnitude of the error between the measured and calculated permeability required the adjustment of the pore aperture radius with a correction factor. This correction factor is a function of pore aperture radius and increases in value as the pore size becomes larger. The correction factor used with the pore aperture radius as measured by the mercury intrusion method will give an effective hydraulic pore aperture radius for use with the Marshall equation.

The correction factor is required because of one important source of error. The pore aperture size calculations are based on the pressure of displacement equation. This equation is based on the geometry of a capillary tube which is not the case in a porous media such as soil.

The correction factor used in this dissertation for pore apertures measured with mercury would not be the same as those measured with water. It is quite possible that pore aperture size distributions measured by water are incorrect because of the non-consideration for primary consolidation and for physical-chemical interactions of the solid particles and the polar liquid, water. Since water has been utilized by most investigators in measuring the relationship between pore aperture size and permeability, these two sources of error have not been serious. One or more of these possible errors may be responsible for the numerous matching factors proposed for

Marshall's equation.

This study has shown that (1) the mercury intrusion porosimeter is a useful instrument in measuring pore size distributions of porous media including agricultural soils, and (2) data from the porosimeter with an adjustment to give the effective hydraulic pore aperture radius, can be used to predict saturated permeabilities of porous media to a high level of accuracy. The results of this study have improved and given a better theoretical basis for using a permeability prediction equation.

BIBLIOGRAPHY

Baver, L. D. 1956. Soil physics. 3d ed. New York, John Wiley and Sons, Inc. 489 p.

Black, C. A. (ed.). 1965. Method of soil analysis. Part I. Agronomy No. 9. Madison, American Society of Agronomy, Inc. 770 p.

Brooks, R. H. and A. T. Corey. 1964. Hydraulic properties of porous media. Fort Collins, Colorado State University. 27 p. (Hydrology Paper no. 3)

Burdine, N. T. 1953. Relative permeability calculations from pore size distribution data. Petroleum Branch, American Institute of Mining and Metallurgical Engineers Transactions, 198:71-78.

Childs, E. C. 1940. The use of soil moisture characteristics in soil studies. Soil Science 50: 239-252.

Childs, E. C. and N. Collis-George. 1950. The permeability of porous materials. Royal Society of London Proceedings, Ser. A, 201: 392-405.

Corey, G. L. 1965. Similitude for non-steady drainage of partially saturated soils. Ph. D. thesis. Fort Collins, Colorado State University. 124 numb. leaves.

Davidson, J. M., J. W. Biggar and D. R. Nielsen. 1963. Transient water flow in unsaturated soils measured by gamma radiation. Journal of Geophysical Research 68: 4777-4783.

Drake, R. L. and L. C. Ritter. 1945a. Pore size distributions in porous materials. Industrial and Engineering Chemistry, Analytical ed., 17:782.

_____ 1945b. Macropore size distributions in some typical porous substances. Industrial and Engineering Chemistry, Analytical ed., 17:787.

Gardner, W. H. and H. E. Fischer. 1966. Concurrent measurement of soil bulk density and water content by attenuation measurement using two gamma energies. Unpublished report prepared at Washington State University, Pullman, Washington for the annual conference on Western Regional Research Project W-68 held at Utah State University, Logan, Utah. 9 numb. leaves.

Gurr, C.G. 1962. Use of gamma rays in measuring water content and permeability in unsaturated columns of soil. Soil Science 94: 224-229.

Hillel, D. and J. Mottes. 1966. Effect of plate impedance, wetting method and aging on soil moisture retention. Soil Science 102: 135-139.

Jackson, R.D., R. J. Reginato and C. H. M. van Bavel. 1965. Comparison of measured and calculated hydraulic conductivities of unsaturated soils. Water Resource Research 1: 375-380.

Kirkham, Don. 1965. Saturated conductivity as a characterizer of soil for drainage design. In: Proceedings of the Drainage for Efficient Crop Production Conference, Chicago, Dec. 6 and 7, 1965. St. Joseph, Michigan, American Society of Agricultural Engineers. p. 24-31.

Leamer, R. W. and J. F. Lutz. 1940. Determination of pore size distribution in soils. Soil Science 49: 347-360.

Laliberte, G. 1966. Properties of unsaturated porous media. Ph. D. thesis. Fort Collins, Colorado State University. 121 numb. leaves.

Marshall, T. J. 1958. A relation between permeability and size distribution of pores. Journal of Soil Science 9: 1-8.

_____ 1959. Relations between water and soil. Harpenden, England, Commonwealth Bureau of Soils. 91 p. (Technical Communication No. 50)

Millington, R. J. and J. P. Quirk. 1959. Permeability of porous media. Nature 183: 387-388.

_____ 1961. Permeability of porous solids. Faraday Society, Transactions 57: 1200-1206.

Miller, E. E. and D. E. Elrick. 1958. Dynamic determination of capillary conductivity extended to non-negligible membrane impedance. Soil Science Society of America, Proceedings 22: 483-486.

Nielsen, D. R. and R. E. Phillips. 1958. Small fritted glass bead plates for determination of moisture retention. Soil Science Society of America, Proceedings 22:574-575.

Nielsen, D. R., Don Kirkham and E. R. Perrier. 1960. Soil capillary conductivity: Comparison of measured and calculated values. Soil Science Society of America, Proceedings 24: 157-160.

Purcell, W. R. 1949. Capillary pressures - Their measurement using mercury and the calculation of permeability therefrom. Petroleum Branch, American Institute of Mining and Metalurgical Engineers, Transactions 186: 39-50.

Richards, L. A. 1941. A pressure-membrane extraction apparatus for soil solution. Soil Science 51: 377-386.

_____ 1948. Porous plate apparatus for measuring moisture retention and transmission by soil. Soil Science 66: 105-110.

_____ 1949. Methods of measuring soil moisture tension. Soil Science 68: 95-112.

Schmidt, R. H. 1961. Hydraulic conductivity and pore size distribution of compacted soils. Master's thesis. Davis, University of California. 83 numb. leaves.

Scholfield, K. A. 1938. Pore size distribution as revealed by the dependence of suction on moisture content. In: Transactions of the First Commission of the International Society of Soil Science. Bangor, Wales, 1938, ed. by G. W. Robinson. Vol A Aberystiryth. p. 54-57.

Stammers, W. N. 1966. The steady state flow of water through unsaturated soil in the low capillary potential region. Ph. D. thesis. Corvallis, Oregon State University. 87 numb. leaves.

Tanner, C. B., S. J. Bourget, and W. E. Holmes. 1954. Moisture tension plates constructed from alundum filter discs. Soil Science Society of America, Proceedings 18: 222-223.

Washburn, E. W. 1921. Note on a method of determining the distribution of pore sizes in a porous media. National Academy of Science, Proceedings 7: 115.

Weast, Robert C. (ed.). 1964. Handbook of Chemistry and Physics. 45th ed. Cleveland, The Chemical Rubber Company. Various paging.

Wyllie, M. R. J. and B. B. Spangler. 1952. Application of electrical resistivity measurements to problems of fluid flow in porous media. American Association of Petroleum Geologist, Bulletin 36: 359-403.

APPENDIX

PORE SIZE DISTRIBUTION DATA

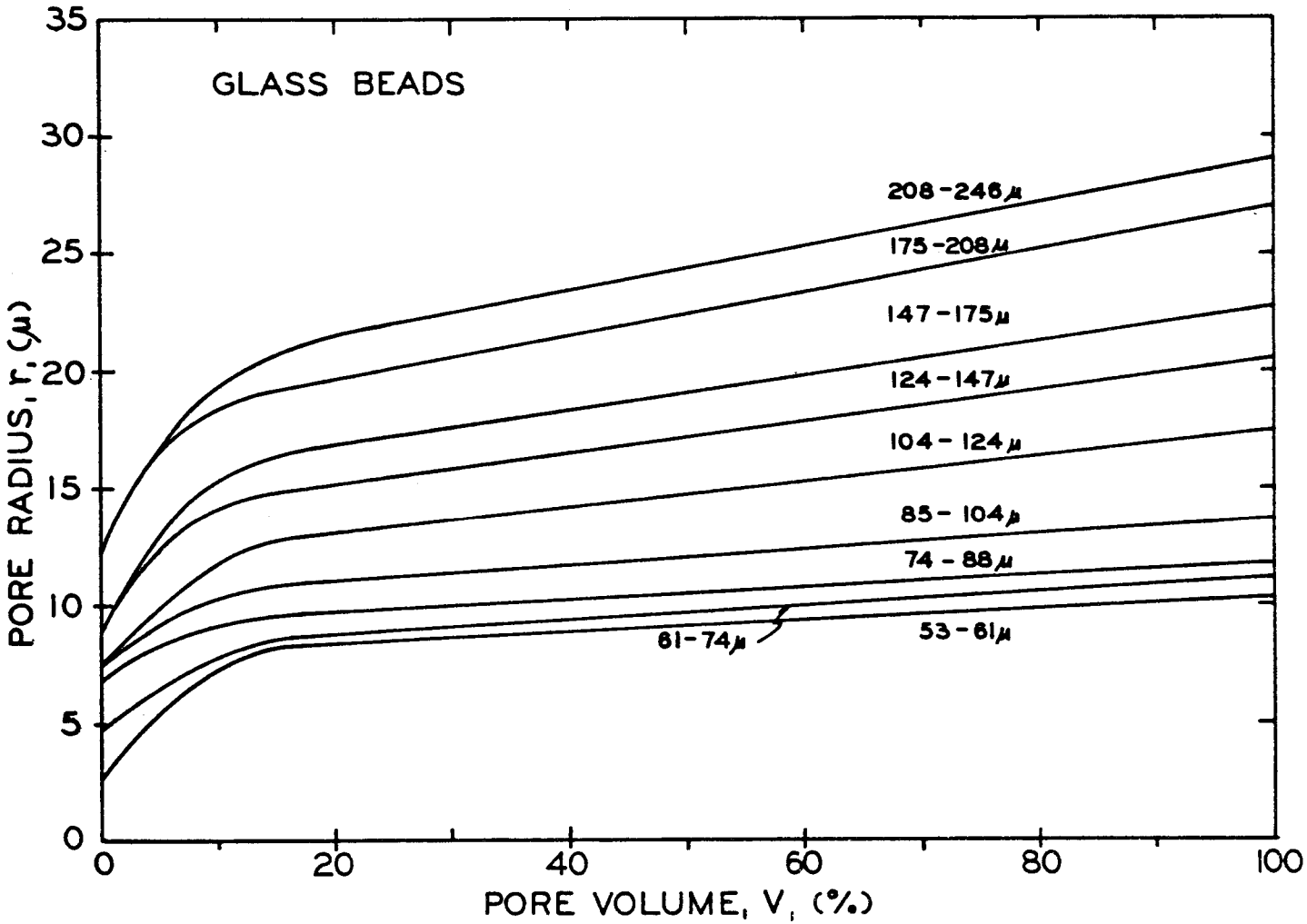

Figure A1. Pore size distributions for the nine sieve classes of glass beads.

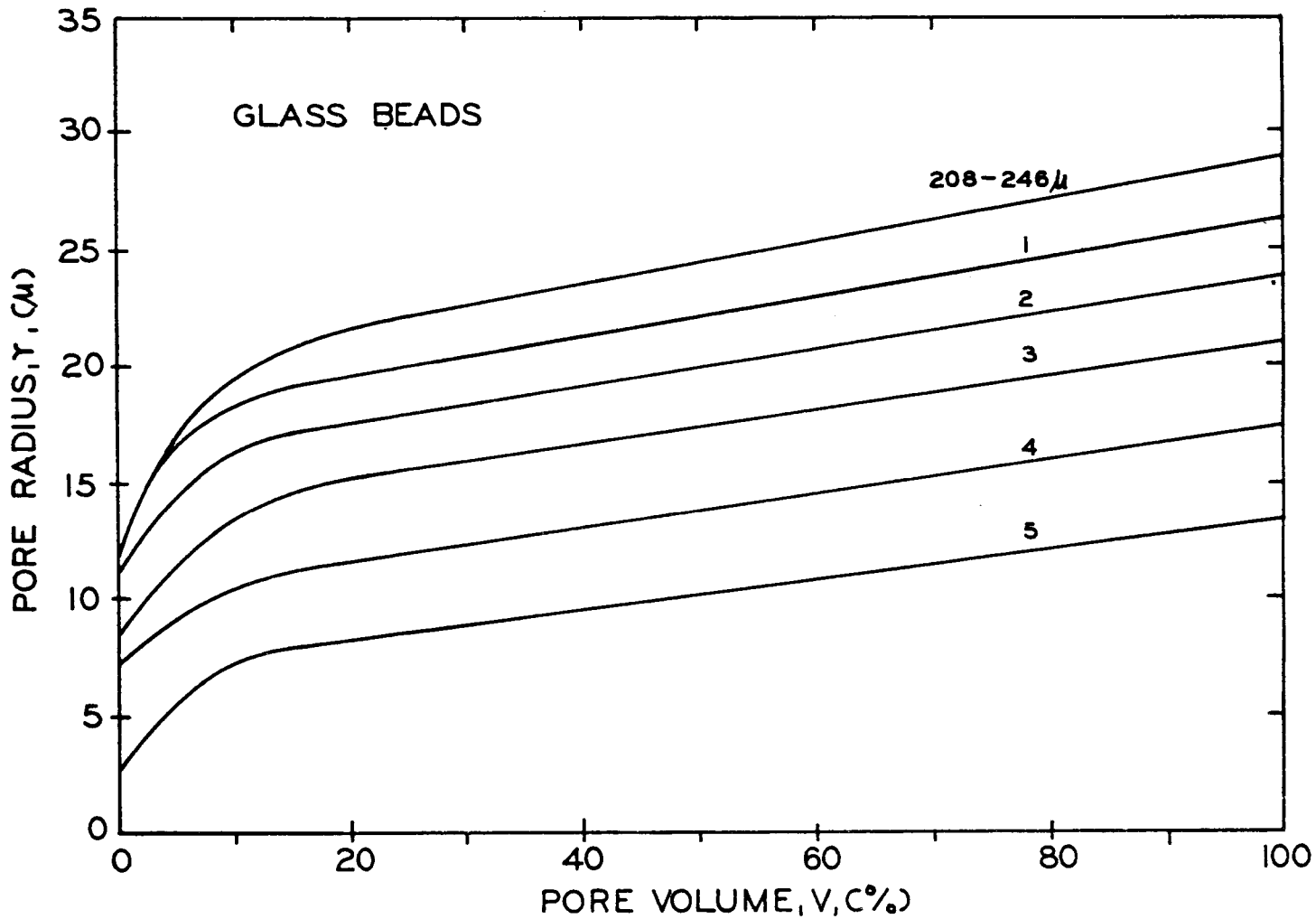

Figure A2. Pore size distribution for glass bead size classes 208-246μ, 1, 2, 3, 4, and 5.

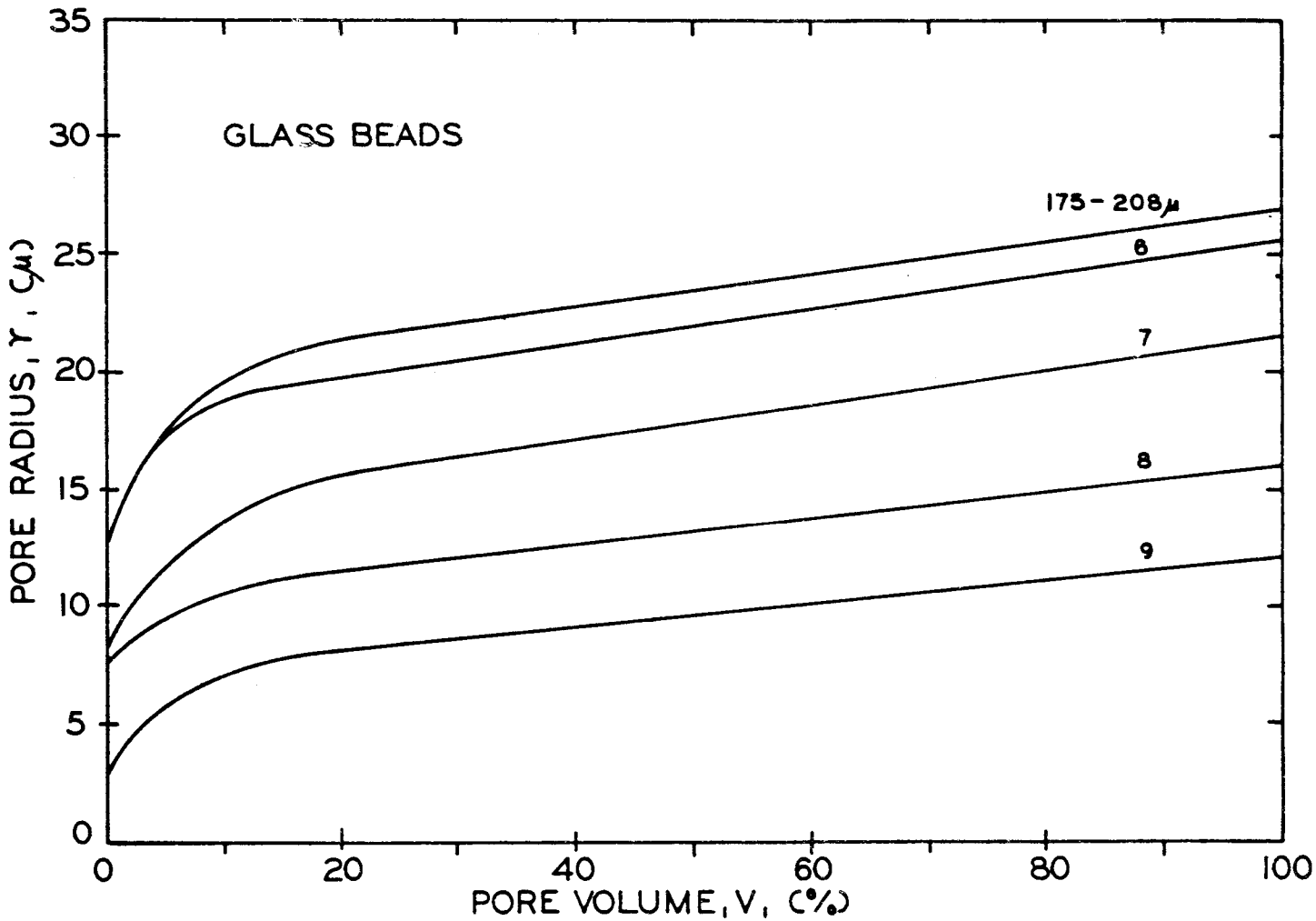

Figure A3. Pore size distribution for glass bead size classes 175-208μ, 6, 7, 8, and 9.

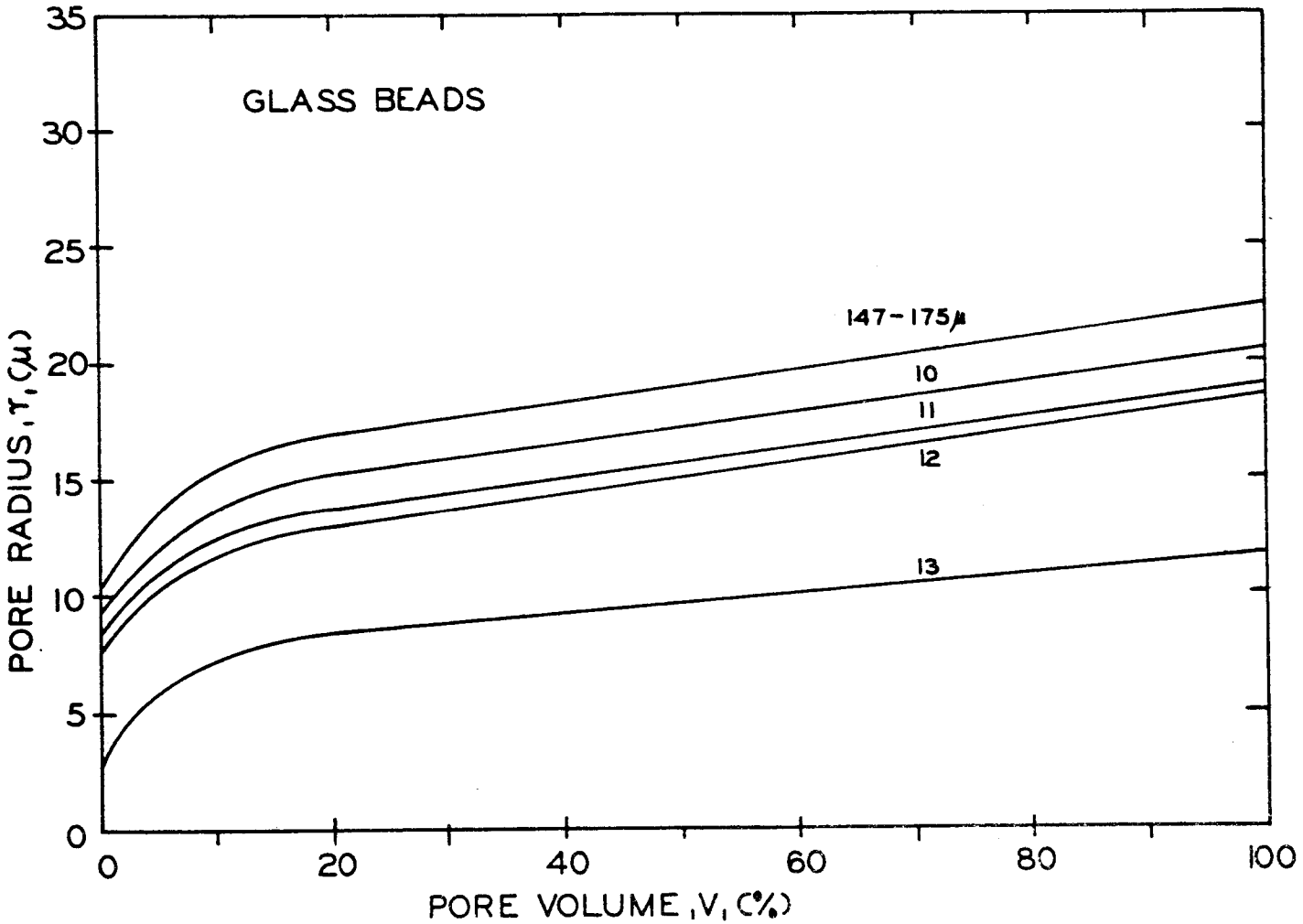

Figure A4. Pore size distribution for glass bead size classes 147-175μ, 10, 11, 12, and 13.

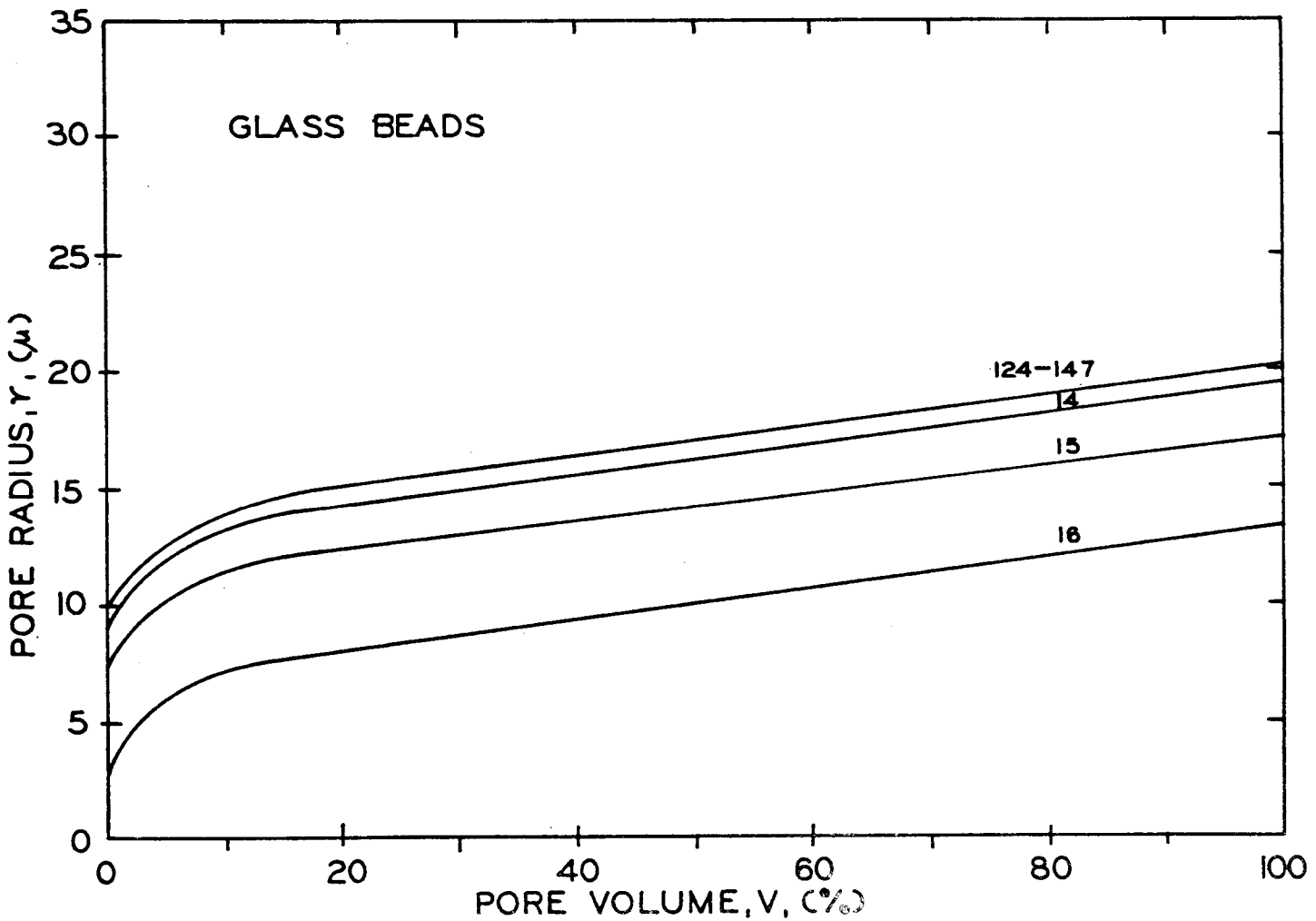

Figure A5. Pore size distribution for glass bead size classes 124-147μ, 14, 15, and 16.

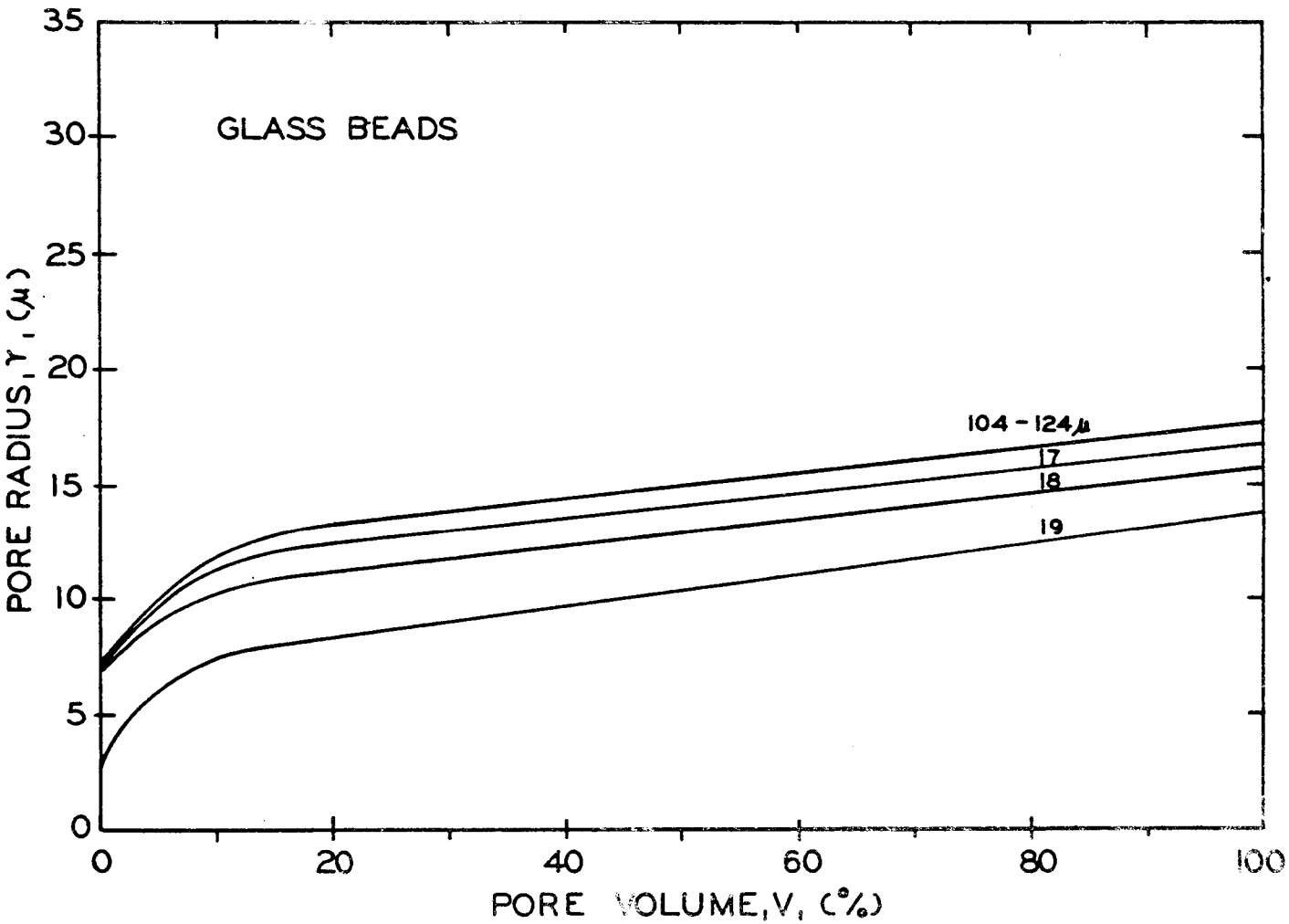

Figure A6. Pore size distribution for glass bead size classes 104-124μ, 17, 18, and 19.

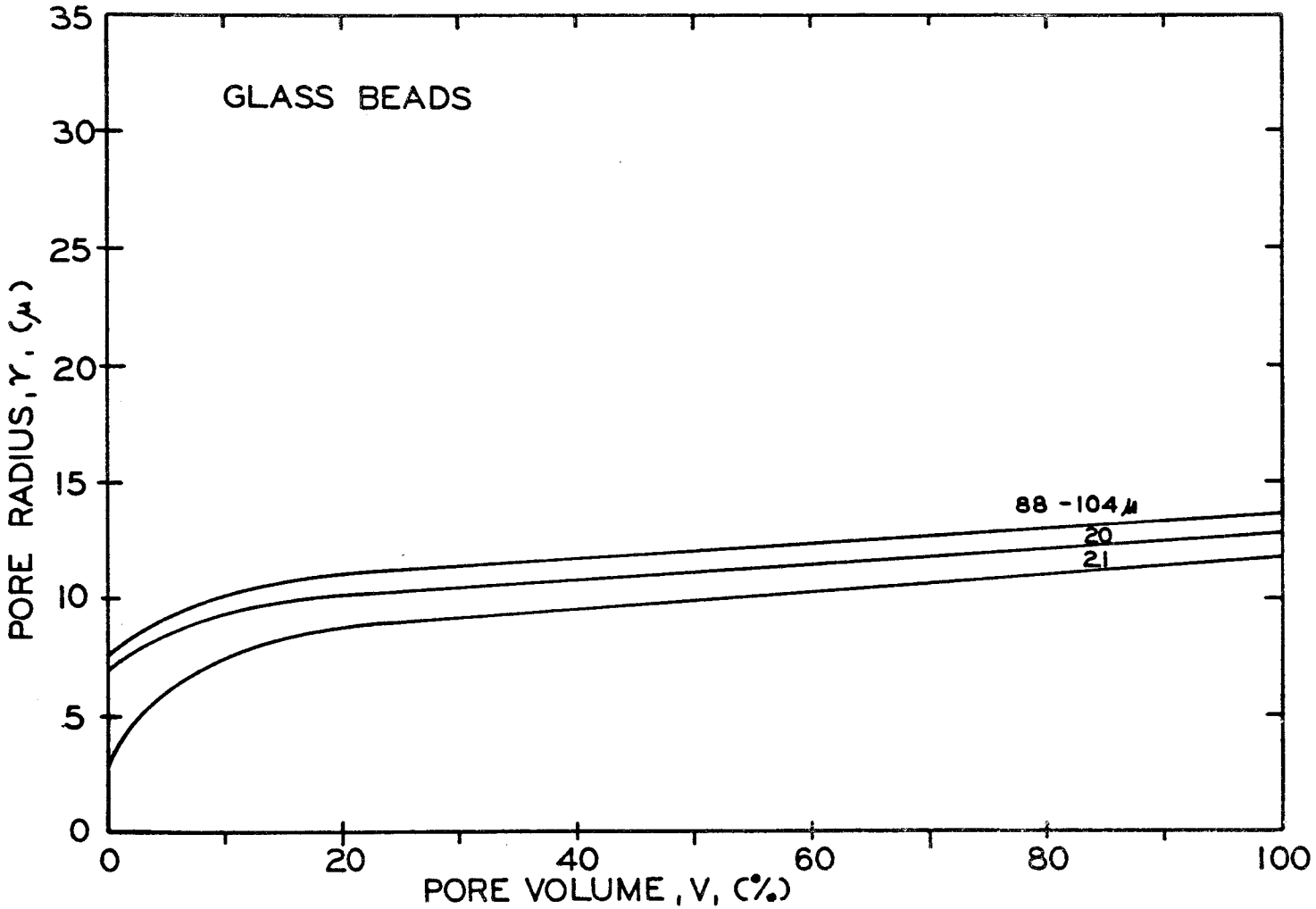

Figure A7. Pore size distribution for glass bead size classes 88-104μ, 20, and 21.

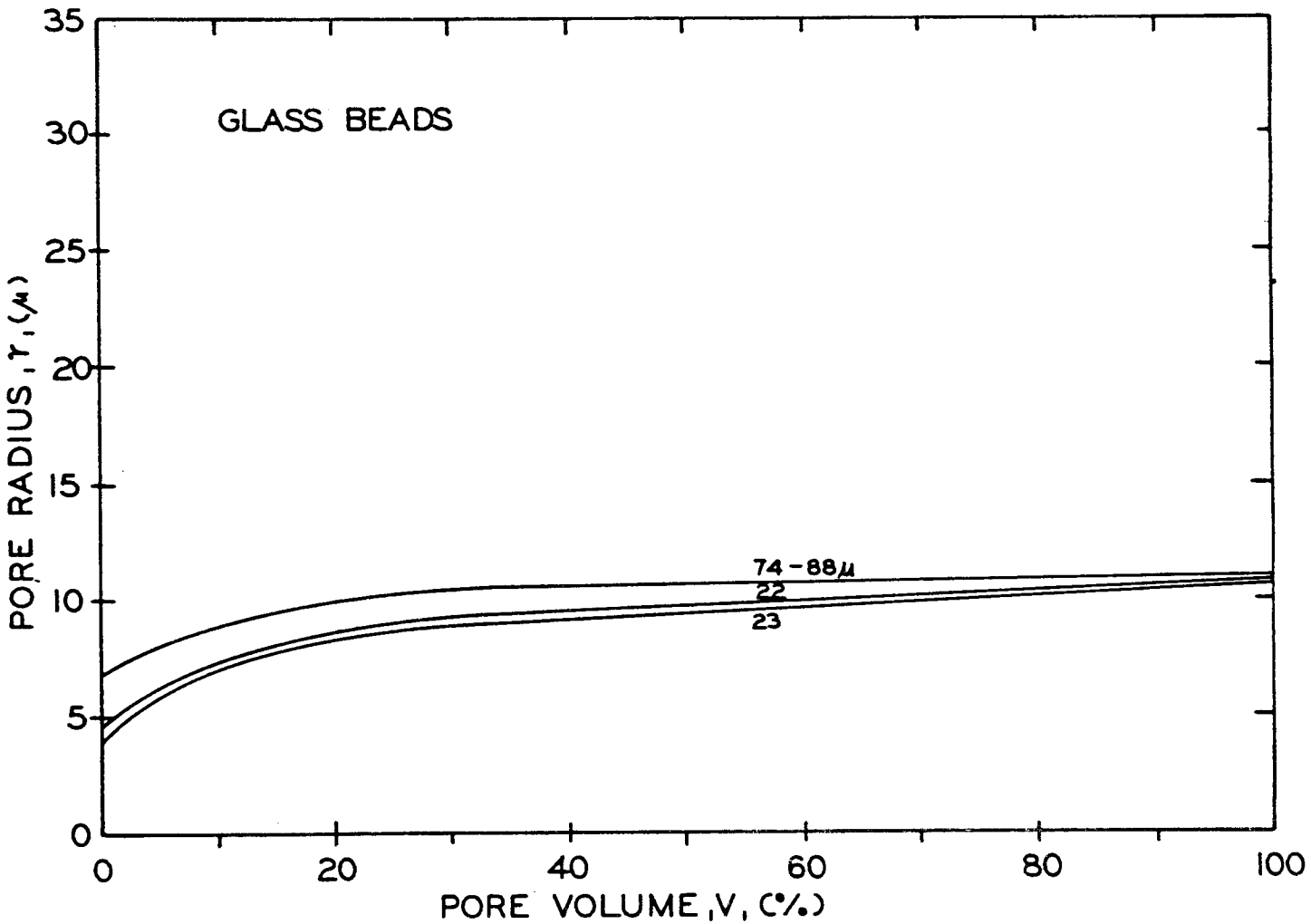

Figure A8. Pore size distribution for glass bead size classes 74-88μ, 22, and 23.

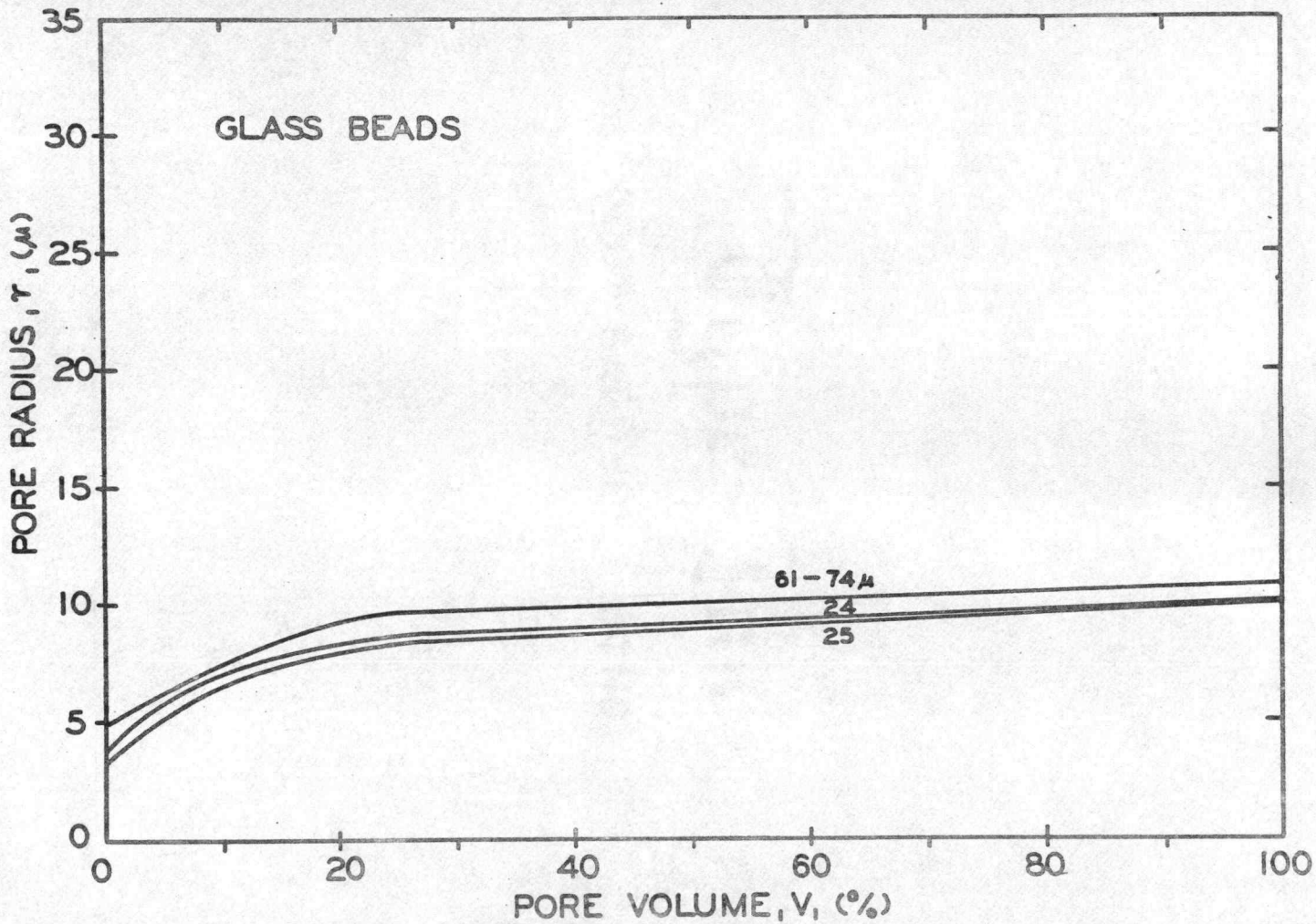

Figure A9. Pore size distribution for glass bead size classes 61-74μ, 24, and 25.

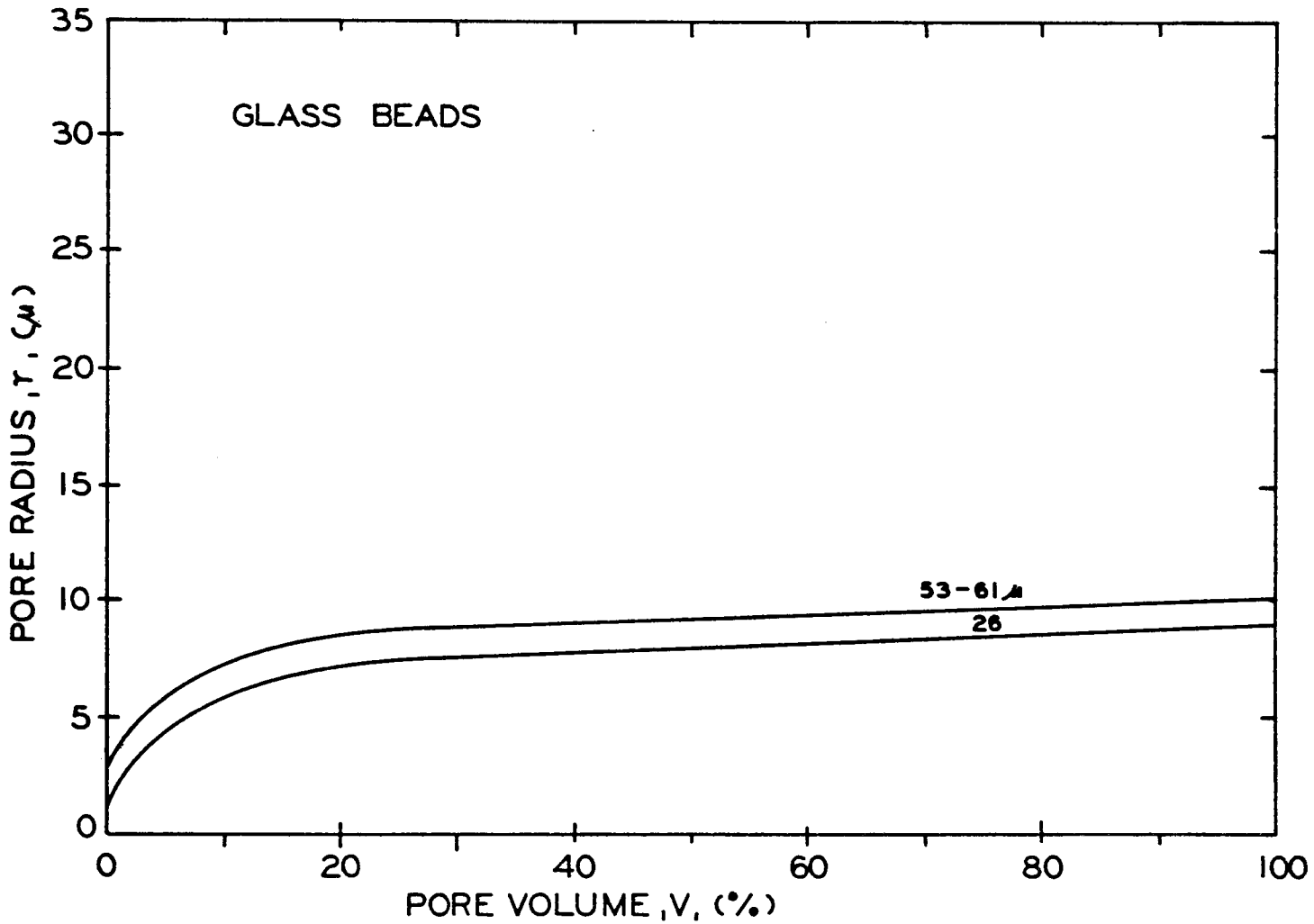

Figure A10. Pore size distribution for glass bead size classes 53-61μ and 26.

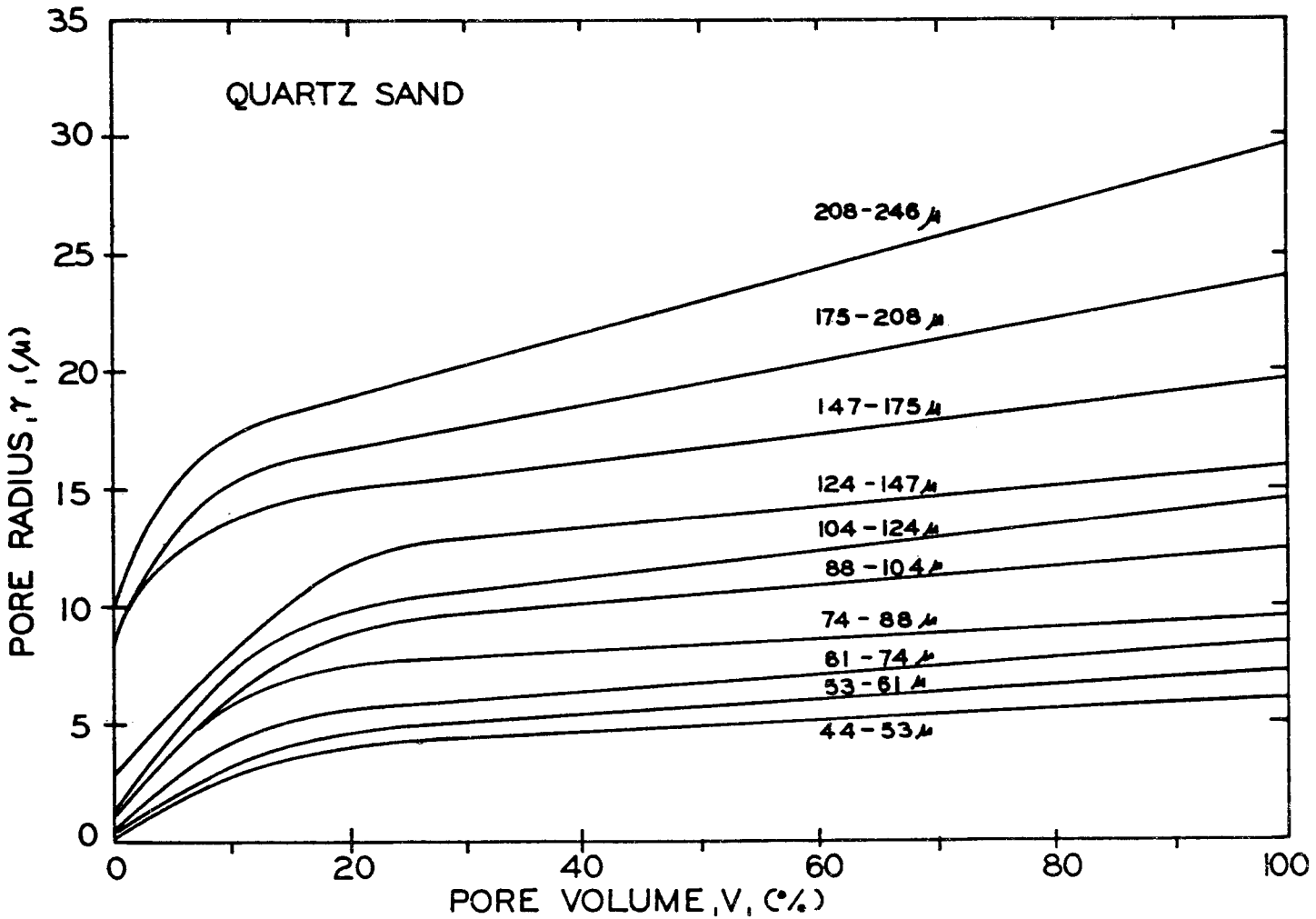

Figure A11. Pore size distribution for the ten sieve size classes of quartz sand.

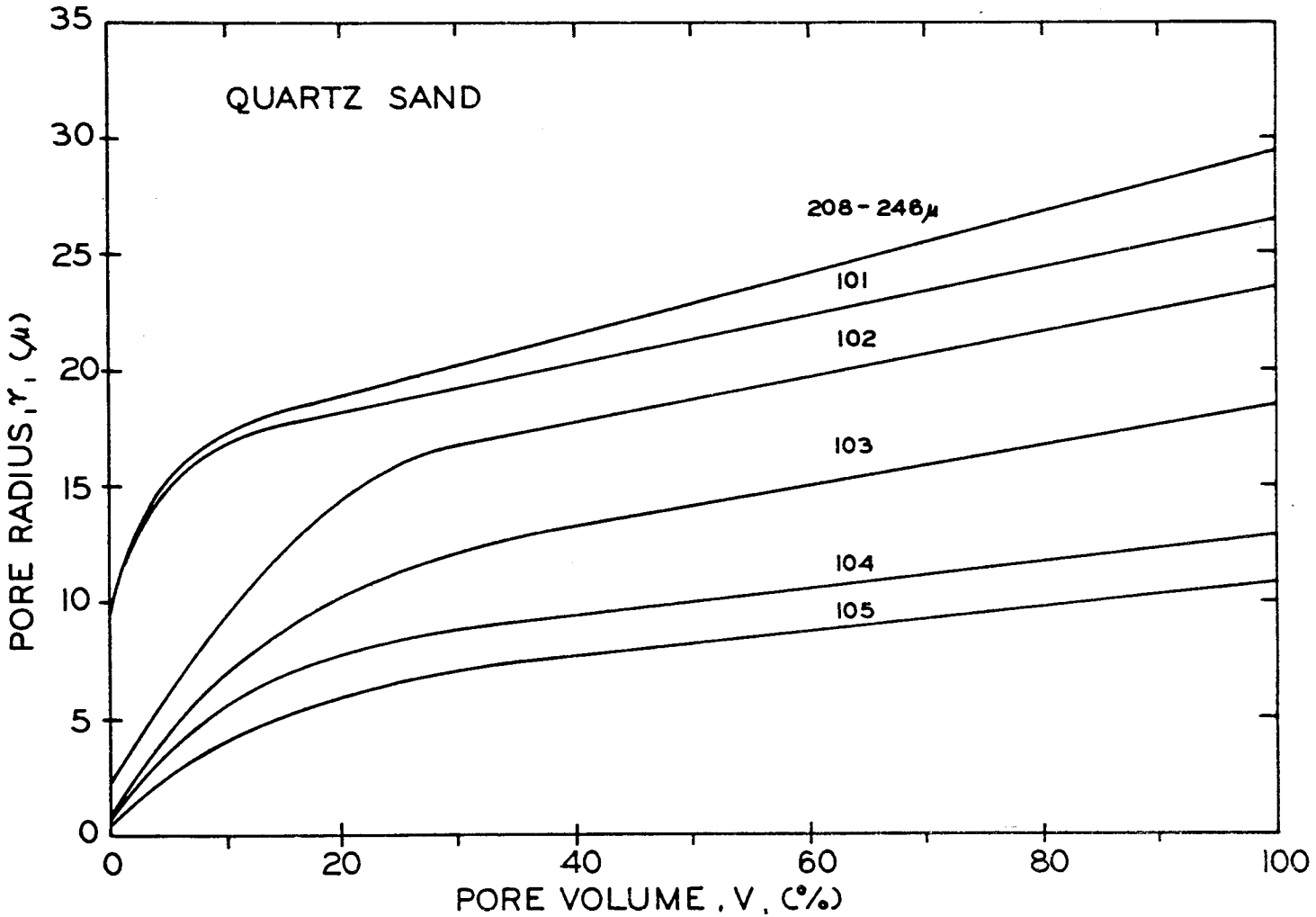

Figure A12. Pore size distribution for quartz sand size classes 208-246μ, 101, 102, 103, 104, and 105.

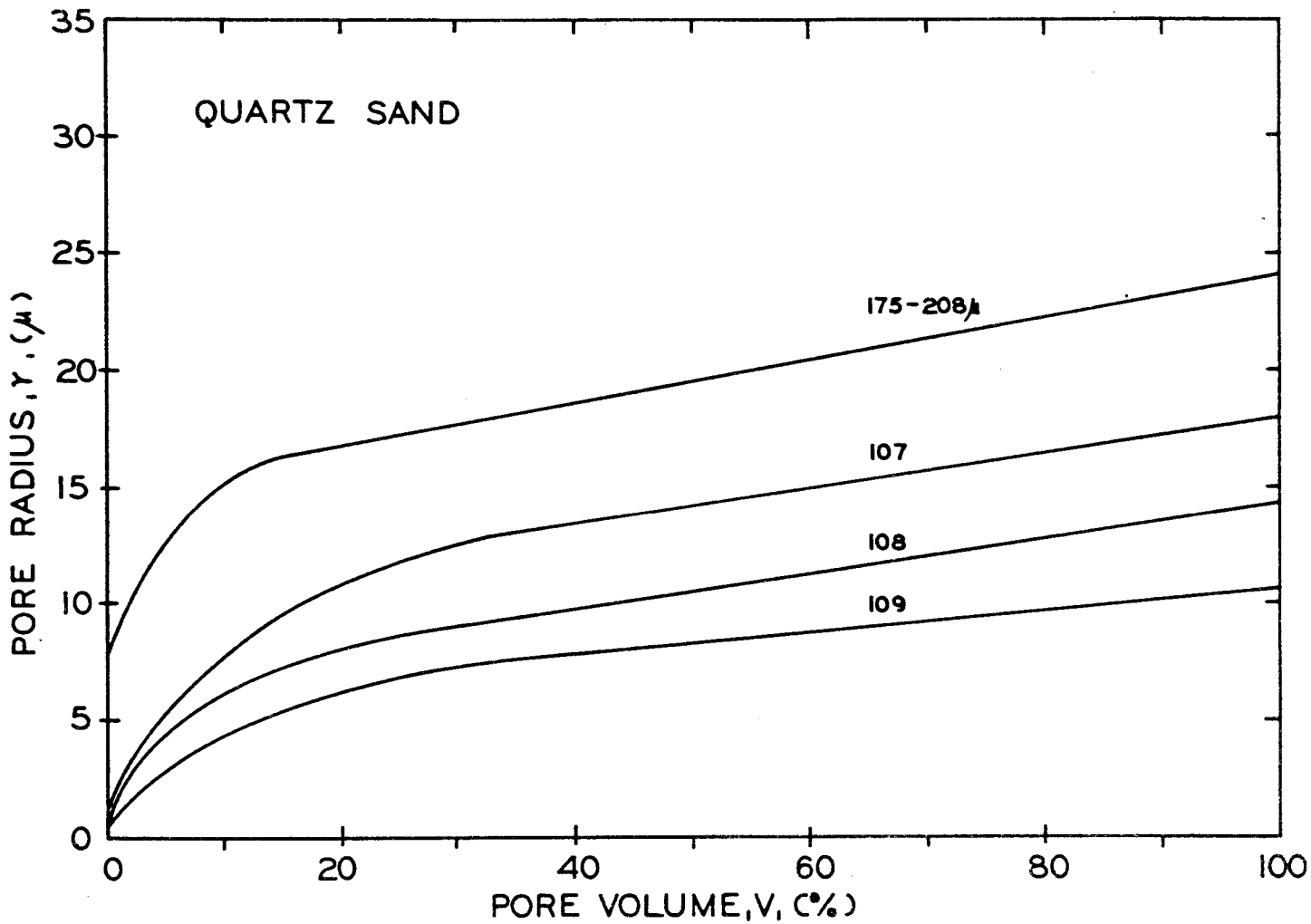

Figure A13. Pore size distribution for quartz sand size classes 175-208μ, 107, 108, and 109.

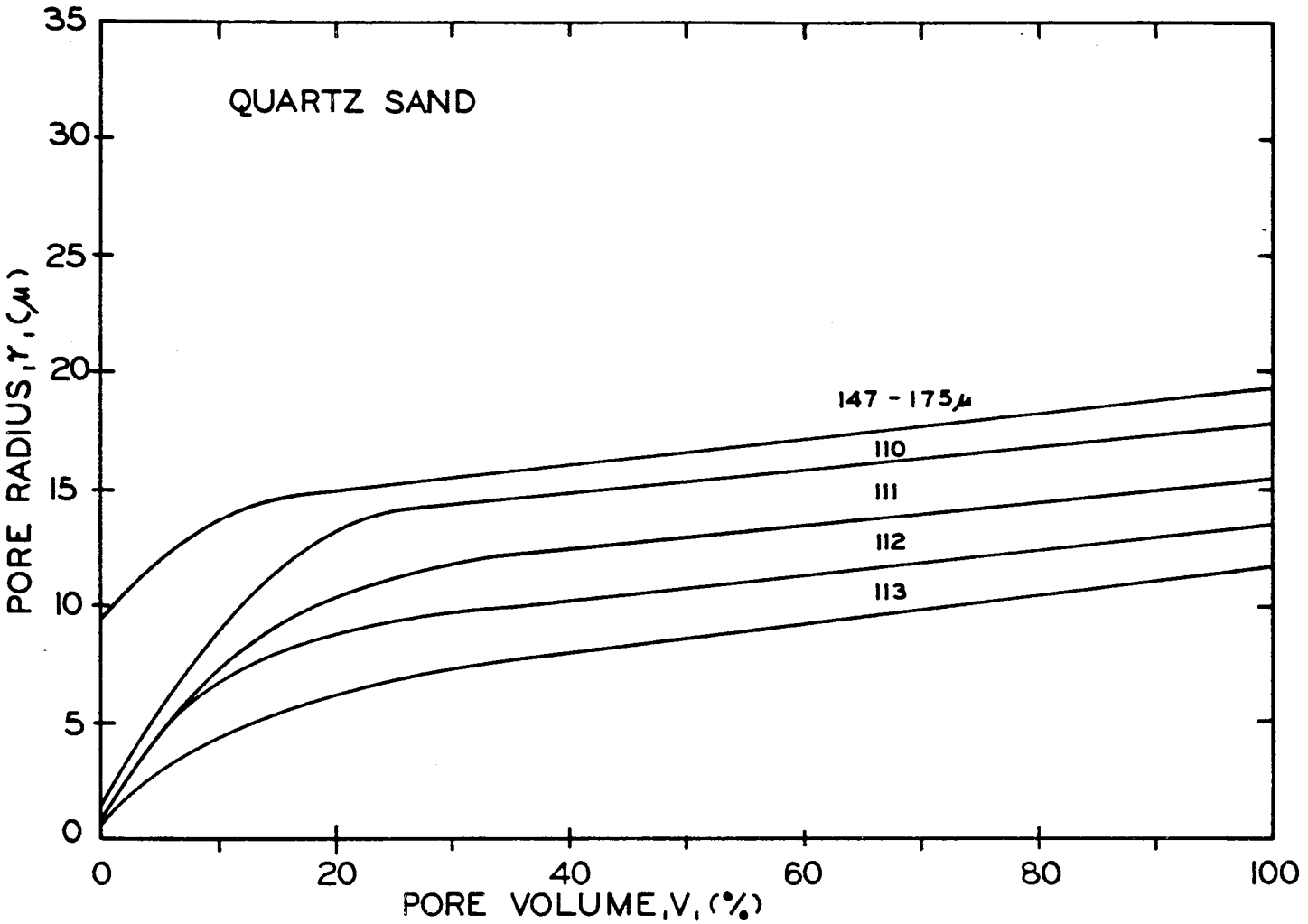

Figure A14. Pore size distribution for quartz sand size classes 147-175μ, 110, 111, 112, and 113.

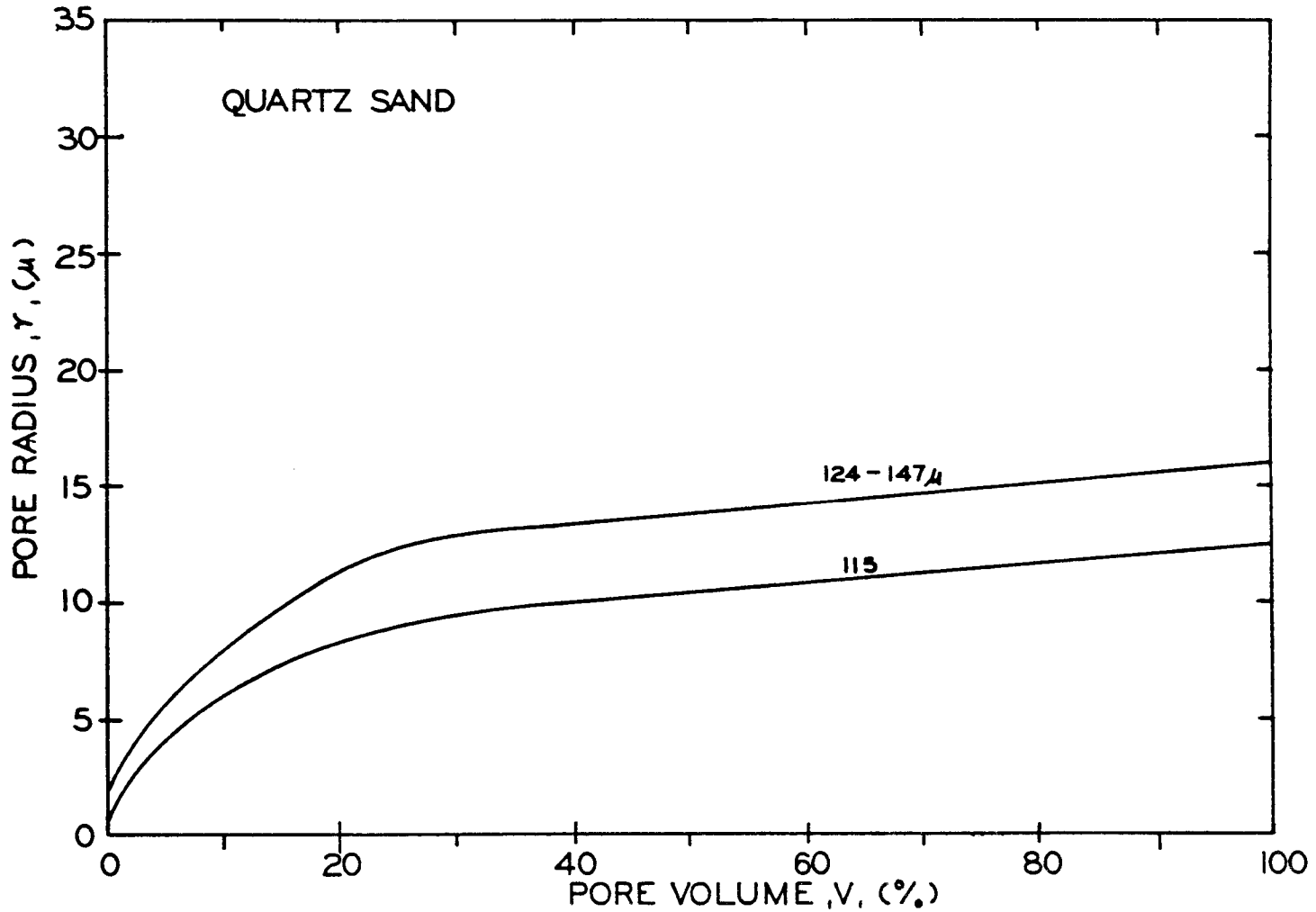

Figure A15. Pore size distribution for quartz sand size classes 124-147μ and 115.

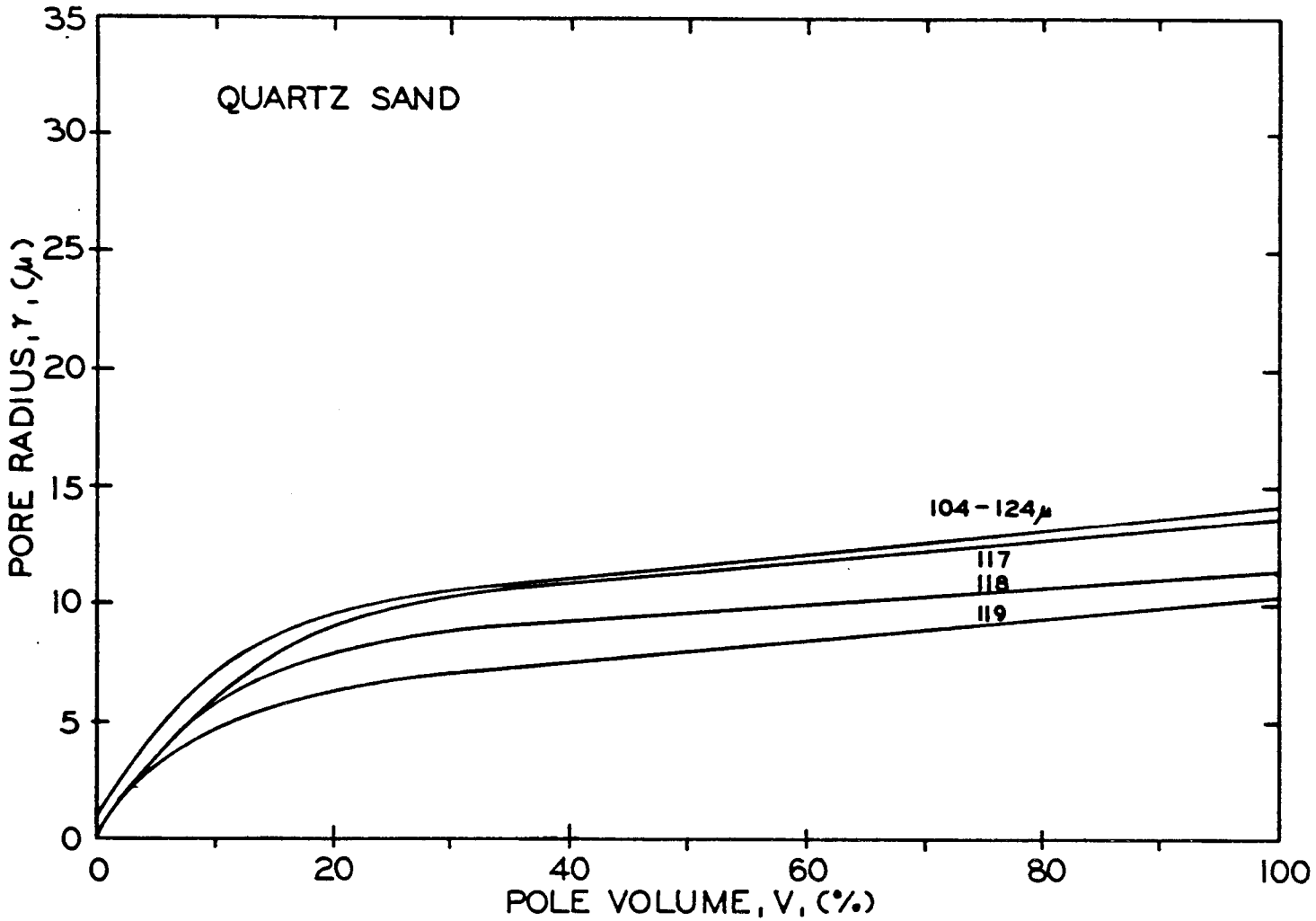

Figure A16. Pore size distribution for quartz sand size classes 104-124μ, 117, 118, and 119.

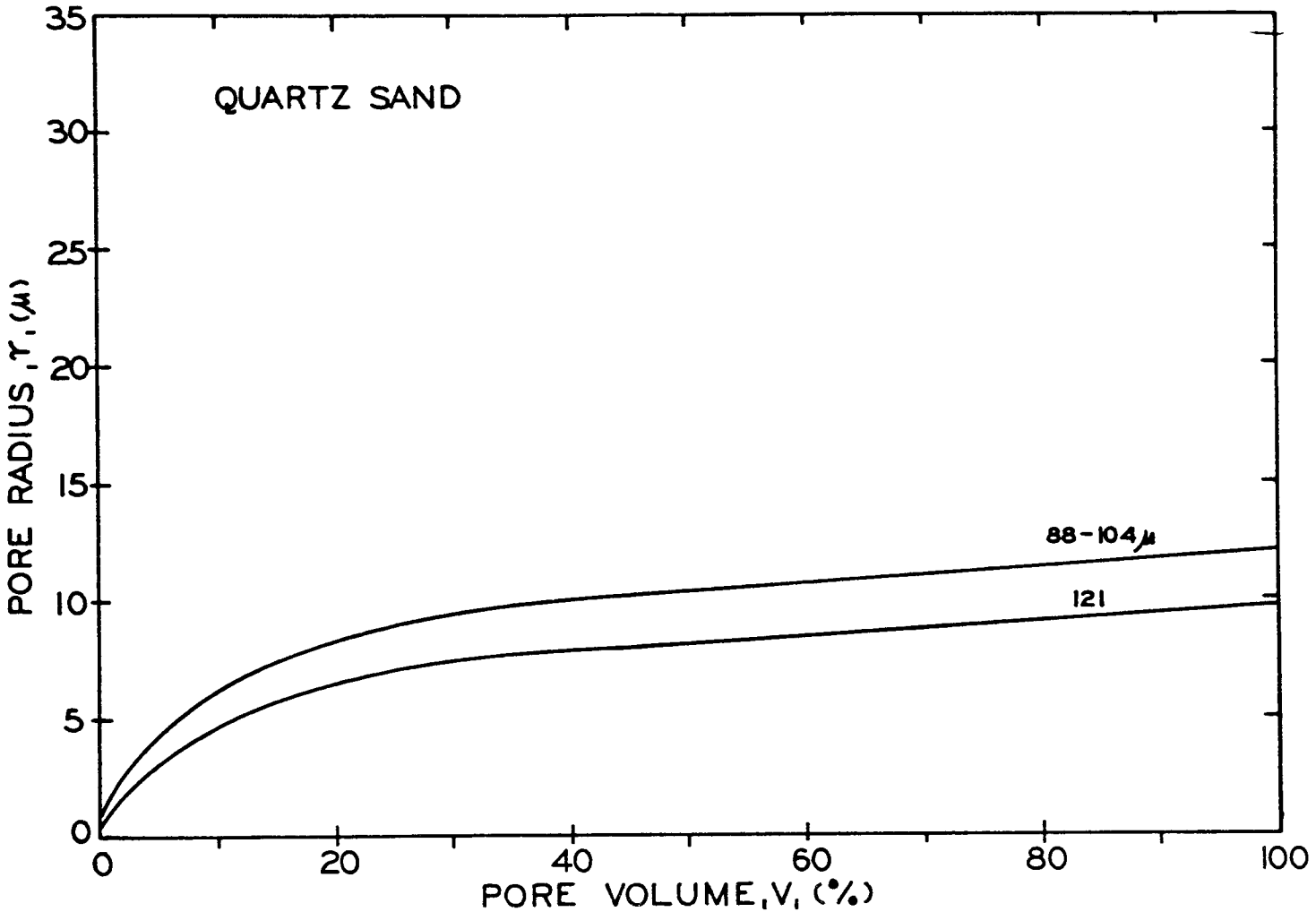

Figure A17. Pore size distribution for quartz sand size classes 88-104μ and 121.

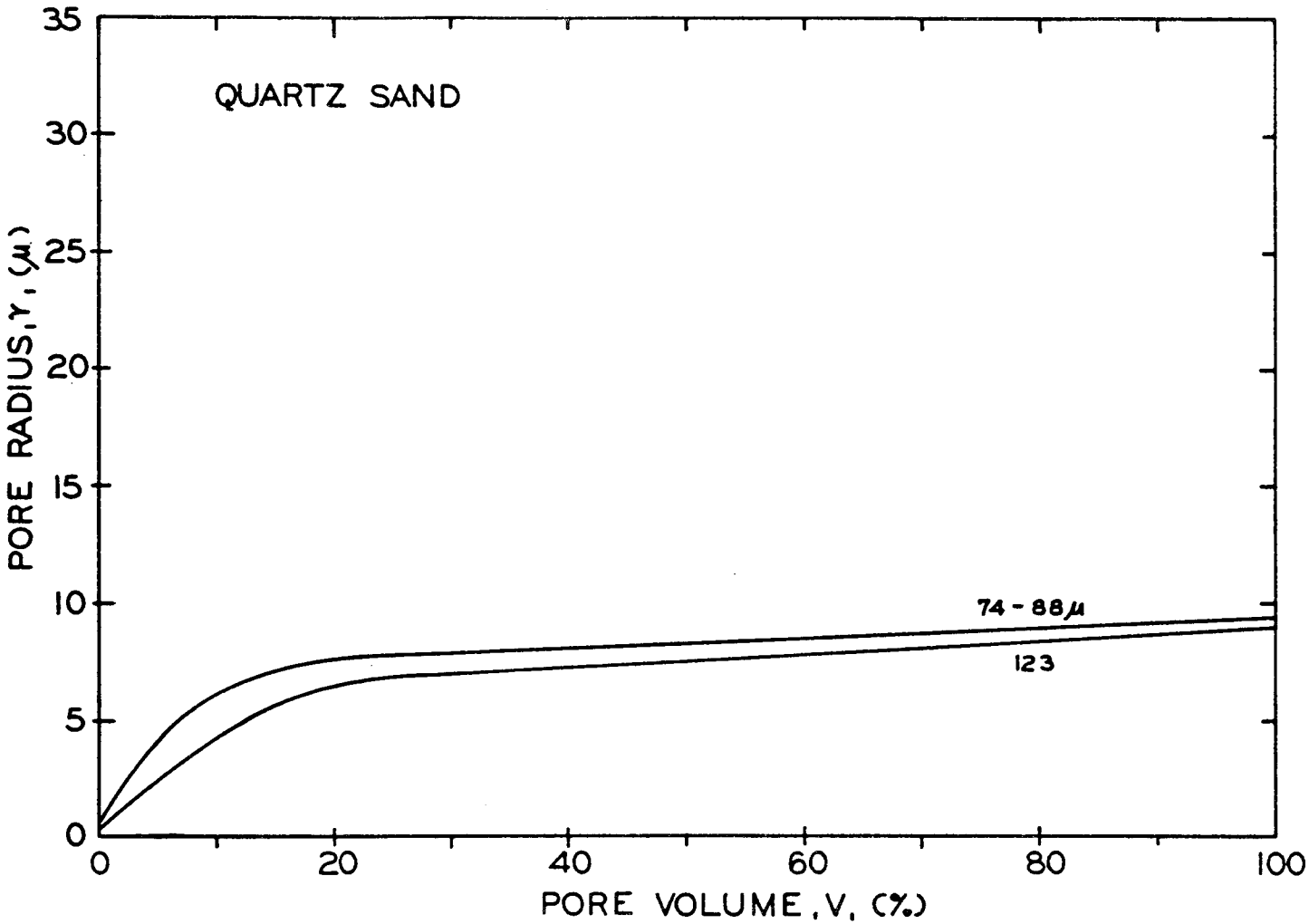

Figure A18. Pore size distribution for quartz sand size classes 74-88μ and 123.

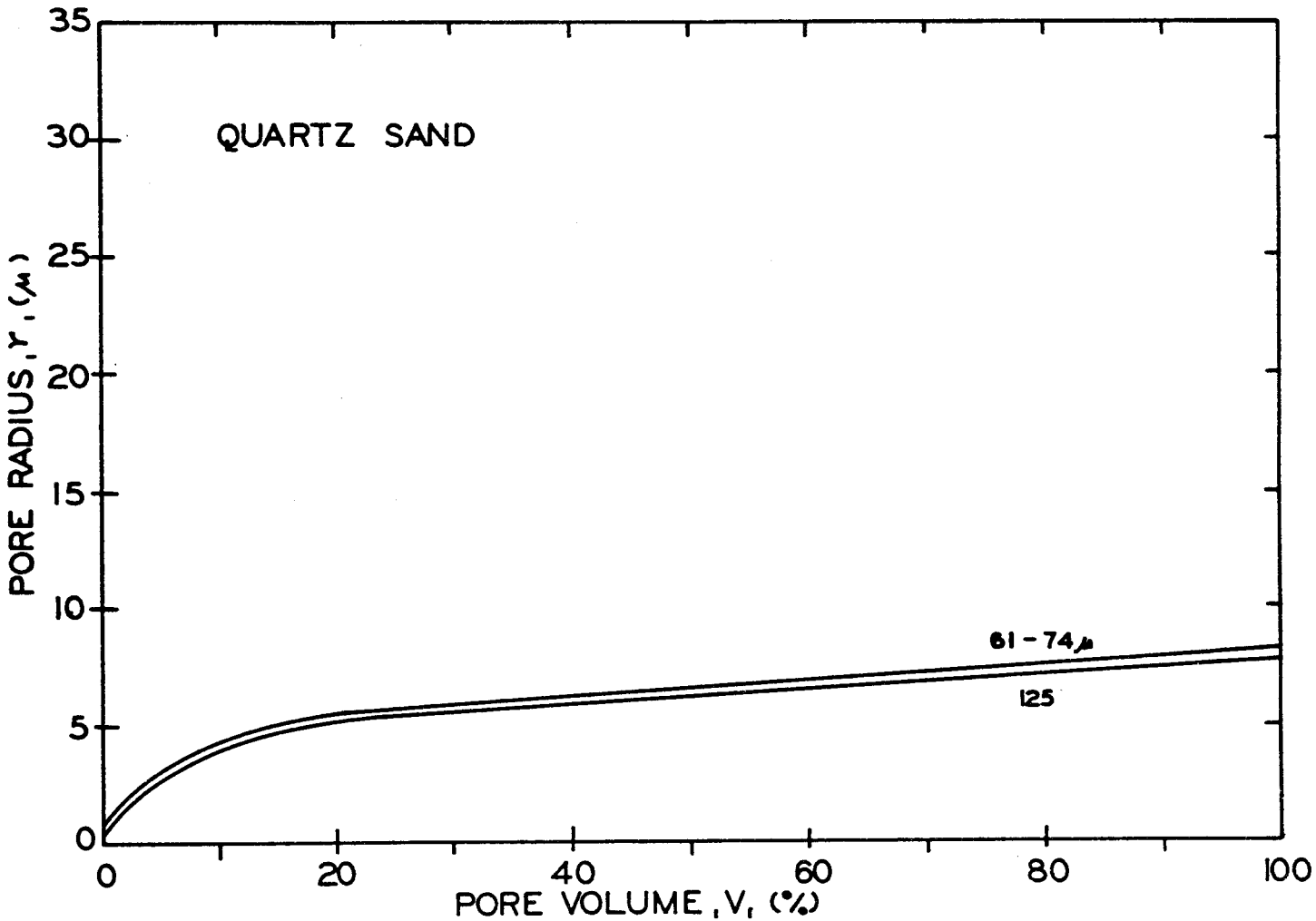

Figure A19. Pore size distribution for quartz sand size classes 61-74μ and 125.